



Semileptonic $B \rightarrow D^{**}$ decays in lattice QCD: a feasibility study and first results

M. Atoui², B. Blossier^{1,a}, V. Morénas², O. Pène¹, K. Petrov³

¹ Laboratoire de Physique Théorique, Unité Mixte de Recherche 8627 du Centre National de la Recherche Scientifique et Université Paris-Sud XI, Bâtiment 210, 91405 Orsay Cedex, France

² Laboratoire de Physique Corpusculaire de Clermont-Ferrand, Unité Mixte de Recherche 6533 CNRS/IN2P3, Université Blaise Pascal, Campus des Cézeaux, 24 avenue des Landais, BP 80026, 63171 Aubière Cedex, France

³ Inria Saclay, Bâtiment Alan Turing, 1 rue Honoré d'Estienne d'Orves, Campus de l'Ecole Polytechnique, 91120 Palaiseau, France

Received: 16 April 2015 / Accepted: 30 July 2015 / Published online: 21 August 2015

© The Author(s) 2015. This article is published with open access at Springerlink.com

Abstract We compute the decays $B \rightarrow D_0^*$ and $B \rightarrow D_2^*$ with finite masses for the b and c quarks. We first discuss the spectral properties of both the B meson as a function of its momentum and the D_0^* and D_2^* at rest. We compute the theoretical formulae leading to the decay amplitudes from the three-point and two-point correlators. We then compute the amplitudes at zero recoil of $B \rightarrow D_0^*$, which turns out not to be vanishing contrary to what happens in the heavy quark limit. This opens the possibility to get better agreement with experiment. To improve the continuum limit we have added a set of data with smaller lattice spacing. The $B \rightarrow D_2^*$ vanishes at zero recoil and we show a convincing signal but only slightly more than 1 sigma from 0. In order to reach quantitatively significant results we plan to exploit fully smaller lattice spacings as well as another lattice regularisation.

1 Introduction

Understanding the composition of the final state in B meson semileptonic decay into charm meson is of key importance to control the theoretical error on the CKM matrix element V_{cb} . The discrepancy between the inclusive determination and the exclusive one, based on $B \rightarrow D^{(*)}l\nu$, is still of the order of 3σ [1]. A significant part of the total width $\Gamma(B \rightarrow X_c l \nu)$ comes from excited states: it was recently argued that the radial excitation D' might be particularly favoured, implying a suppression of the $B \rightarrow D^*$ form factors as suggested by a study performed using the operator product expansion formalism [2]. Another group of states that contribute to the width, about one quarter of it, is orbital excitations, in other words, positive parity charmed mesons, that we will note D^{**} hereafter. They are not well understood: indeed there

seems to be a persistent discrepancy between claims from theory and from experiment [3], while a comparison between semileptonic decay and non-leptonic decay $B \rightarrow D^{**}\pi$, involving the same form factors (at least in the case of the so-called Class I process), is quite confusing on the experimental side [4]. Two types of D^{**} are observed: two “narrow resonances” $D_{3/2}$ and a couple of “broad resonances” $D_{1/2}$, in the same mass region [5]. While experiments point towards a dominance of the broad resonances in semileptonic decays, theory points rather towards the dominance of the narrow resonances: not only a series of sum rules [6, 7] derived from QCD obtains that hierarchy, but also calculations with quark models [8–10] and lattice computations performed in the quenched approximation [11] and with $N_f = 2$ dynamical quarks [12]. However, the main limitation of these results is that they are derived in the heavy quark limit. $1/m_c$ corrections might be pretty large and, before getting any definitive conclusion on the disagreement between theory and experiment in that sector of flavour physics, it is mandatory to reduce the sources of systematic errors on the theory side.

2 Theoretical framework

In this paragraph, all the main formulae up to the differential decay rates will be given for the semileptonic decays of a B heavy meson into the first orbitally excited D^{**} mesons.

We will focus our study on the production of the $|^3P_0\rangle$ (scalar D_0^*) and the $|^3P_2\rangle$ (tensor D_2^*) states.¹

Finally, we will also give relations in the case where the mass of the lepton cannot be neglected.

¹ We use the $|^{2S+1}L_J\rangle$ notation of the states, where S is the spin angular momentum, $L = 1$ the orbital angular momentum and $J = L + S$ the total angular momentum of the D^{**} state.

^a e-mail: benoit.blossier@th.u-psud.fr

2.1 Form factors

In order to derive the decay rates, we need the transition amplitudes. They can be described using six form factors [15]:

3P_2 state

$$\begin{aligned} & \langle {}^3P_2(p_{D_2^*}, \varepsilon(p_{D_2^*}, \lambda)) | V_\mu | B(p_B) \rangle \\ &= i [\tilde{h}] \epsilon_{\mu\nu\lambda\rho} \varepsilon_{(p_{D_2^*}, \lambda)}^{*\nu\alpha} p_{B\alpha} (p_B + p_{D_2^*})^\lambda (p_B - p_{D_2^*})^\rho, \\ & \langle {}^3P_2(p_{D_2^*}, \varepsilon(p_{D_2^*}, \lambda)) | A_\mu | B(p_B) \rangle \\ &= [\tilde{k}] \varepsilon_{\mu\nu}^{*(p_{D_2^*}, \lambda)} p_B^\nu + \left(\varepsilon_{\alpha\beta}^{*(p_{D_2^*}, \lambda)} p_B^\alpha p_B^\beta \right) \\ & \quad \times \left[\tilde{b}_+ (p_B + p_{D_2^*})_\mu + \tilde{b}_- (p_B - p_{D_2^*})_\mu \right], \end{aligned} \quad (2.1)$$

3P_0 state

$$\begin{aligned} & \langle {}^3P_0(p_{D_0^*}) | V_\mu | B(p_B) \rangle = 0 \quad (\text{parity invariance}), \\ & \langle {}^3P_0(p_{D_0^*}) | A_\mu | B(p_B) \rangle = [\tilde{u}_+] (p_B + p_{D_0^*})_\mu \\ & \quad + [\tilde{u}_-] (p_B - p_{D_0^*})_\mu \end{aligned} \quad (2.2)$$

where V_μ denotes the vector current $\bar{c}\gamma_\mu b$ and A_μ the axial current $\bar{c}\gamma_\mu\gamma_5 b$.

$\varepsilon(p_{D_2^*}, \lambda)$ is the polarisation tensor of the 3P_2 state (λ being the projection of the $J = 2$ total angular momentum along some quantification axis).

Moreover, the chosen normalisation of the mesonic states is

$$\langle M(p') | M(p) \rangle = (2\pi)^3 2E \delta^3(\vec{p}' - \vec{p}).$$

Finally, because of parity and time-reversal invariance of the strong interactions, those form factors are real numbers.

2.2 Differential decay rates

The goal is to compute the differential decay width $d\Gamma(\bar{B} \rightarrow D^{**} \ell \bar{\nu})$ whose general expression is

$$d\Gamma(\bar{B} \rightarrow D^{**} \ell \bar{\nu}) = \frac{1}{2E_B} |\mathcal{M}|^2 d\Phi,$$

with

$$\begin{aligned} & d\Phi = \frac{d^3\vec{p}_{D^{**}}}{(2\pi)^3 2E_{D^{**}}} \frac{d^3\vec{p}_\ell}{(2\pi)^3 2E_\ell} \frac{d^3\vec{p}_\nu}{(2\pi)^3 2E_\nu} (2\pi)^4 \delta^{(4)}(p_B - p_{D^{**}} - p_\ell - p_\nu), \\ & |\mathcal{M}|^2 = \sum_{\mu, \nu} W_{\mu\nu} \ell^{\mu\nu}. \end{aligned}$$

In the last equality, $W_{\mu\nu}$ denotes the hadronic tensor

$$\begin{aligned} W_{\mu\nu}(p_B, p_{D^{**}}) &= \frac{G_F^2 |V_{cb}|^2}{2} \\ & \times \sum_{\text{final spins}} \langle D^{**}(p_{D^{**}}) | V_\mu - A_\mu | \bar{B}(p_B) \rangle \\ & \times \langle \bar{B}(p_B) | V_\nu - A_\nu | D^{**}(p_{D^{**}}) \rangle, \end{aligned}$$

where the transition amplitudes have been given in the preceding paragraph (let us note that there are no summation nor average over the initial spins since the \bar{B} meson has a spin equal to 0) and $\ell^{\mu\nu}$ represents the leptonic tensor

$$\begin{aligned} \ell^{\mu\nu}(p_\ell, p_\nu) &= \sum_s [\bar{u}_\ell(p_\ell, s) \gamma^\mu (1 - \gamma^5) v_\nu(p_\nu)] \\ & \quad \cdot [\bar{u}_\ell(p_\ell, s) \gamma^\nu (1 - \gamma^5) v_\nu(p_\nu)]^*. \end{aligned}$$

In that last formula, $u_\ell(p_\ell, s)$ is the lepton ℓ spinor (s denotes the usual projection of its spin), while $v_\nu(p_\nu)$ represents the antineutrino $\bar{\nu}$ spinor.

All that remains is to compute the leptonic tensor, and then the hadronic tensor and the measure $d\Phi$ of the phase space in order to obtain the expressions of the differential decay widths.

2.2.1 Leptonic tensor $\ell^{\mu\nu}$

The calculation is classical and straightforward, leading to

$$\begin{aligned} \ell^{\mu\nu} &= 8[p_\ell^\mu p_\nu^\nu + p_\ell^\nu p_\nu^\mu - (p_\ell \cdot p_\nu) g^{\mu\nu} \\ & \quad - i \epsilon^{\mu\nu\rho\sigma} (p_\ell)_\rho (p_\nu)_\sigma]. \end{aligned}$$

We notice that the mass of the lepton has vanished, which renders the expression valid in the situations where $m_\ell = 0$ as well as $m_\ell \neq 0$.

2.2.2 Hadronic tensor $W_{\mu\nu}$

By looking at the expressions of the transition amplitudes given above, the general structure of the hadronic tensor can be inferred and put into the form [15]

$$\begin{aligned}
W_{\mu\nu} = & \frac{G_F^2 |V_{cb}|^2}{2} \\
& \times \left[\boxed{\alpha} g_{\mu\nu} + \boxed{\beta_{++}} (p_B + p_{D^{**}})_\mu (p_B + p_{D^{**}})_\nu \right. \\
& + \boxed{\beta_{+-}} (p_B + p_{D^{**}})_\mu (p_B - p_{D^{**}})_\nu \\
& + \boxed{\beta_{-+}} (p_B - p_{D^{**}})_\mu (p_B + p_{D^{**}})_\nu \\
& + \boxed{\beta_{--}} (p_B - p_{D^{**}})_\mu (p_B - p_{D^{**}})_\nu \\
& \left. + i \boxed{\gamma} \epsilon_{\mu\nu\rho\sigma} (p_B + p_{D^{**}})^\rho (p_B - p_{D^{**}})^\sigma \right]. \quad (2.3)
\end{aligned}$$

The coefficients α , β_{++} , β_{+-} , β_{-+} , β_{--} and γ are given in the “Appendix” for the 3P_0 and the 3P_2 states.

2.2.3 Kinematics and notations

For reasons of simplicity, we now choose to compute the decay rates in the rest frame of the \bar{B} meson.

We then define two dimensionless parameters x and y according to

$$\boxed{x m_B = 2 E_\ell} \quad \text{as well as} \quad \boxed{y m_B^2 = (p_B - p_{D^{**}})^2 = (p_\ell + p_\nu)^2}$$

where E_ℓ is the energy of the lepton in the \bar{B} rest frame.

We introduce also the mass ratio r_X

$$\boxed{m_X = r_X m_B} \quad \text{where } X \text{ is either a } D^{**} \text{ meson or the lepton } \ell.$$

Many kinematical terms can be expressed with these three parameters, such as

$$\begin{aligned}
E_{D^{**}} &= \frac{m_B}{2} (1 - y + r_{D^{**}}^2); \quad p_\ell \cdot p_\nu = \frac{1}{2} m_B^2 (y - r_\ell^2); \\
p_\ell \cdot p_{D^{**}} &= \frac{1}{2} m_B^2 (x - y - r_\ell^2); \quad p_B \cdot p_\ell = \frac{1}{2} m_B^2 x.
\end{aligned}$$

2.2.4 Measure $d\Phi$ of the phase space

The goal is to get the differential widths $d\Gamma$ with respect to the lepton energy E_ℓ and the momentum transfer $(p_B - p_{D^{**}})^2$, in other words with respect to the variables x and y : $d^2\Gamma/dx dy$.

So we must integrate over the antineutrino momentum \vec{p}_ν , then over all possible orientations of \vec{p}_ℓ , so that only the dependence on E_ℓ (i.e. on x) remains, and finally over all possible directions of the three-vector $\vec{p}_{D^{**}}$, since we want to keep the dependence on $E_{D^{**}}$ (i.e. on y). We finally get:

$$d\Phi = - \frac{m_B^2}{128\pi^3} dx dy \theta(1 - x + y - r_{D^{**}}^2)$$

where $\theta(z)$ is the usual Heaviside function.

2.2.5 Constraints on x and y

The parameters x and y , that is, the lepton energy (E_ℓ) and the D^{**} meson energy ($E_{D^{**}}$), cannot be arbitrary. They are

constrained by two conditions: one which is obvious in the expression of $d\Phi$ above (the Heaviside function) and another one which appeared during the integration over the direction of \vec{p}_ℓ . In other words, we have access to the variation domains of both parameters x and y whether we consider $x = x(y)$ or $y = y(x)$: they are given in the “Appendix”.

2.2.6 Differential decay widths in the \bar{B} rest frame

Using the definition of $d\Gamma$ as well as all the preceding results, the construction of the differential decay widths proceeds in the following way:

$$\frac{d\Gamma}{dx dy} (\bar{B} \rightarrow D^{**} \ell \bar{\nu}) = - \frac{m_B}{256\pi^3} |\mathcal{M}|^2$$

where $|\mathcal{M}|^2 = W_{\mu\nu} \ell^{\mu\nu}$ becomes in this particular frame

$$\begin{aligned}
|\mathcal{M}|^2 = & 2 G_F^2 |V_{cb}|^2 m_B^2 \left\{ -2 \boxed{\alpha} (y - r_\ell^2) \right. \\
& - \boxed{\beta_{++}} m_B^2 [4 [x r_{D^{**}}^2 + (1 - x)(y - x)] \\
& + r_\ell^2 [3 y - 4(x + r_{D^{**}}^2) + r_\ell^2]] \\
& + \left(\boxed{\beta_{+-}} + \boxed{\beta_{-+}} \right) m_B^2 r_\ell^2 [2(1 - x - r_{D^{**}}^2) + y + r_\ell^2] \\
& + \boxed{\beta_{--}} m_B^2 r_\ell^2 (y - r_\ell^2) \\
& \left. - 2 \boxed{\gamma} m_B^2 [y (1 + y - 2x - r_{D^{**}}^2) + r_\ell^2 (1 + y - r_{D^{**}}^2)] \right\}.
\end{aligned}$$

We notice that, for a zero mass lepton, only the coefficients α , β_{++} and γ survive.

The expressions for each D^{**} are also written in the “Appendix”. However, their use requires the knowledge of the momentum dependence of the form factors. In the following, we will focus on a method to obtain such a dependence.

2.3 Extracting the form factors from the transition amplitudes

On the lattice, we compute the transition amplitudes for different momenta of the mesons. But we need the momentum dependence of the form factors in order to calculate the decay rates of the semileptonic decays of the B to a D^{**} . So we must devise a way to extract the form factors from the lattice transition amplitudes.

2.3.1 Kinematics

We will work in the rest frame of the D^{**} meson² so the B meson will carry the momentum. Moreover, we will consider the B 's whose spatial momentum is symmetrical.

$$p_{D^{**}} = (m_{D^{**}}, \vec{0}) \quad \text{and} \quad p_B^\mu = (E_B, p, p, p).$$

² This will greatly simplify the calculations on the lattice.

We will also choose the Minkowski metric: $g_{\mu\nu} = \text{Diag}(+, -, -, -)$.

The other piece we need is the expression of the polarisation tensor for the 3P_2 state in the D^{**} rest frame, that is, $\varepsilon(\vec{0}, \lambda)$. We can construct it from the combination of two spin-1 states,

$$\varepsilon^{\mu\nu}(\vec{0}, \lambda) = \sum_{s, s'} \langle 1 \ 1 \ s \ s' | 2 \ \lambda \rangle \varepsilon^\mu(\vec{0}, s) \varepsilon^\nu(\vec{0}, s'),$$

where the Clebsch–Gordan coefficients for $1+1 \rightarrow 2$ appear as well as the polarisation vector $\varepsilon^\mu(\vec{0}, s)$ of a spin-1 state. The final expressions are gathered in the “Appendix”.

2.3.2 3P_0 form factors

Using the notation

$$\mathcal{T}_\mu^A \stackrel{\text{def.}}{=} \langle ^3P_0 A_\mu B(p_B) \rangle,$$

we explicitly get from Eq. (2.2):

$$\begin{cases} \mathcal{T}_0^A = \boxed{\tilde{u}_+}(E_B + m_{D^{**}}) + \boxed{\tilde{u}_-}(E_B - m_{D^{**}}) \\ \quad \text{(temporal direction),} \\ \mathcal{T}_i^A = \boxed{\tilde{u}_+}p + \boxed{\tilde{u}_-}p \quad \text{(spatial direction).} \end{cases}$$

So it is straightforward to express \tilde{u}_+ and \tilde{u}_- with the \mathcal{T}_μ^A 's. The results are presented in the “Appendix”.

2.3.3 3P_2 form factors

In the following, we will adopt the notation

$$\mathcal{T}_{\mu(\lambda)}^A \stackrel{\text{def.}}{=} \langle ^3P_2(\lambda) A_\mu B(p_B) \rangle \quad \text{as well as}$$

$$\mathcal{T}_{\mu(\lambda)}^V \stackrel{\text{def.}}{=} \langle ^3P_2(\lambda) V_\mu B(p_B) \rangle.$$

In order to extract one particular form factor, we can choose in Eq. (2.1) either some spatial direction where each coefficient of the other form factors vanishes, or we can construct a linear combination of the $\mathcal{T}_{i(\lambda)}^A$ and/or the $\mathcal{T}_{i(\lambda)}^V$.

This procedure can be carried out by using the expressions for the polarisation tensor and the four-momenta at our disposal and calculating the contribution of the corresponding terms appearing in the matrix elements (2.1) which define the form factors (those contributions are gathered in Table 1).

A few possibilities are collected in the “Appendix”.

2.4 Summary

We have constructed all the theoretical formulae which allow us to calculate the decay widths of the semileptonic $B \rightarrow D^{**}$ channels. The strategy to use them is the following:

Table 1 Contributions of the polarisation tensor in the $B \rightarrow ^3P_2$ transition amplitude

$\varepsilon_{\mu\nu}^{(\lambda)}$	$\varepsilon_{\mu\nu}^{(\lambda)} p_B^\nu$
$\varepsilon_{\mu\nu}^{(+2)}$	$\frac{p}{2}(0, 1+i, i-1, 0)$
$\varepsilon_{\mu\nu}^{(+1)}$	$-\frac{p}{2}(0, 1, i, 1+i)$
$\varepsilon_{\mu\nu}^{(0)}$	$-\frac{p}{\sqrt{6}}(0, 1, 1, -2)$
$\varepsilon_{\mu\nu}^{(-1)}$	$\frac{p}{2}(0, 1, -i, 1-i)$
$\varepsilon_{\mu\nu}^{(-2)}$	$\frac{p}{2}(0, 1-i, -1-i, 0)$
$\varepsilon_{\mu\nu}^{(+2)} + \varepsilon_{\mu\nu}^{(-2)}$	$p(0, 1, -1, 0)$
$\varepsilon_{\mu\nu}^{(+2)} - \varepsilon_{\mu\nu}^{(-2)}$	$p(0, i, i, 0)$
$\varepsilon_{\mu\nu}^{(+1)} + \varepsilon_{\mu\nu}^{(-1)}$	$p(0, 0, -i, -i)$
$\varepsilon_{\mu\nu}^{(+1)} - \varepsilon_{\mu\nu}^{(-1)}$	$p(0, -1, 0, -1)$
$\varepsilon_{\mu\nu}^{(\lambda)}$	$\varepsilon_{\mu\nu}^{(\lambda)} p_{B\ \nu}$
$\varepsilon_{(+2)}^{\mu\nu}$	$-\frac{p}{2}(0, 1+i, -1+i, 0)$
$\varepsilon_{(+1)}^{\mu\nu}$	$\frac{p}{2}(0, 1, i, 1+i)$
$\varepsilon_{(0)}^{\mu\nu}$	$\frac{p}{\sqrt{6}}(0, 1, 1, -2)$
$\varepsilon_{(-1)}^{\mu\nu}$	$\frac{p}{2}(0, -1, i, -1+i)$
$\varepsilon_{(-2)}^{\mu\nu}$	$\frac{p}{2}(0, -1-i, 1-i, 0)$
$\varepsilon_{(+2)}^{\mu\nu} + \varepsilon_{(-2)}^{\mu\nu}$	$p(0, -1, 1, 0)$
$\varepsilon_{(+2)}^{\mu\nu} - \varepsilon_{(-2)}^{\mu\nu}$	$p(0, -i, -i, 0)$
$\varepsilon_{(+1)}^{\mu\nu} + \varepsilon_{(-1)}^{\mu\nu}$	$p(0, 0, i, i)$
$\varepsilon_{(+1)}^{\mu\nu} - \varepsilon_{(-1)}^{\mu\nu}$	$p(0, 1, 0, 1)$
$\varepsilon_{(\lambda)}^{\mu\nu}$	$\varepsilon_{(\lambda)}^{\mu\nu} p_{B\ \mu} p_{B\ \nu}$
$\varepsilon_{(+2)}^{\mu\nu}$	ip^2
$\varepsilon_{(+1)}^{\mu\nu}$	$-(1+i)p^2$
$\varepsilon_{(0)}^{\mu\nu}$	0
$\varepsilon_{(-1)}^{\mu\nu}$	$(1-i)p^2$
$\varepsilon_{(-2)}^{\mu\nu}$	$-ip^2$
$\varepsilon_{(+2)}^{\mu\nu} + \varepsilon_{(-2)}^{\mu\nu}$	0
$\varepsilon_{(+2)}^{\mu\nu} - \varepsilon_{(-2)}^{\mu\nu}$	$2ip^2$
$\varepsilon_{(+1)}^{\mu\nu} + \varepsilon_{(-1)}^{\mu\nu}$	$-2ip^2$
$\varepsilon_{(+1)}^{\mu\nu} - \varepsilon_{(-1)}^{\mu\nu}$	$-2p^2$

1. Compute, on the lattice, the transition amplitudes for the $B \rightarrow D^{**}$ processes.
2. Extract the form factors from them.
3. Use the formulae in the “Appendix” to obtain the decay widths.

Since we expect the lattice 3P_2 computation to be somewhat tricky, we are first going to estimate the contribution of the \tilde{k} , \tilde{b}_+ , \tilde{b}_- and \tilde{h} form factors to the $\bar{B} \rightarrow D_2^* \ell \bar{\nu}$ decay width.

2.5 Estimation of the contribution of the form factors to the 3P_2 decay width

There are four form factors needed to describe the transition amplitudes from a B to a 3P_2 state which increases the difficulty in the lattice computations. So it could be useful to have an idea of each of their contribution to the decay widths.

In order to get a quantitative hint, we will relate these form factors to their infinite mass limit $\tau_{3/2}$ and use this $\tau_{3/2}$ to produce a numerical estimation.

2.5.1 Infinite mass limit

In the limit where the heavy quark of the meson has an infinite mass, new symmetries (and thus additional conserved quantities) appear. These new symmetries provide additional relations between the transition amplitudes so that the form factors become dependent. It can be proven [13] that this reduction of the form factors leads to the following relations for the 3P_2 state:

$$\begin{cases} \tilde{h} = \frac{\sqrt{3}}{2} \frac{1}{m_B^2 \sqrt{r_{D_2^*}}} \tau_{3/2} & \tilde{k} = \sqrt{3} \sqrt{r_{D_2^*}} (1+w) \tau_{3/2} \\ \tilde{b}_+ = -\frac{\sqrt{3}}{2} \frac{1}{m_B^2 \sqrt{r_{D_2^*}}} \tau_{3/2} & \tilde{b}_- = \frac{\sqrt{3}}{2} \frac{1}{m_B^2 \sqrt{r_{D_2^*}}} \tau_{3/2} \end{cases}$$

where the parameter w is defined by

$$m_B m_{D_2^*} w = p_B \cdot p_{D_2^*} \implies \boxed{y = 1 + r_{D_2^*}^2 - 2 r_{D_2^*} w}$$

and $\tau_{3/2}$ is one of the so-called Isgur–Wise functions.

2.5.2 Fit of $\tau_{3/2}$

Using a covariant construction of the transition amplitudes in the infinite mass limit (quark models à la Bakamjian–Thomas), it has been shown [8, 14] that the Isgur–Wise function $\tau_{3/2}$ can be well fitted by

$$\begin{aligned} \tau_{3/2}(w) &= \tau_{3/2}(1) \left(\frac{2}{1+w} \right)^{2\sigma_{3/2}} \\ \implies \tau_{3/2}(y) &= \tau_{3/2}(1) \left[\frac{4 r_{D_2^*}}{(1+r_{D_2^*})^2 - y} \right]^{2\sigma_{3/2}} \end{aligned}$$

where the accessible phase space domain is given by

$$1 \leq w \leq \frac{m_B^2 + m_{D_2^*}^2}{2 m_B m_{D_2^*}} \implies (1 - r_{D_2^*})^2 \geq y \geq 0.$$

We will also take (GI model [15] in [8]):

$$\tau_{3/2}(1) \simeq 0.54 \quad \text{as well as} \quad \sigma_{3/2}^2 \simeq 1.50.$$

2.5.3 Quantitative prediction of each contribution to the total width

We are now in a position to estimate the contribution of each form factor to the total width of the $\bar{B} \rightarrow D_2^* \ell \bar{\nu}$ decay channel. Let us take the case of a zero mass lepton to simplify the calculations. Starting from the expression of $\frac{d^2\Gamma}{dx dy}$ and with the notations given in the “Appendix”, we can perform both the integrations over x and over y and we get:

C_i	$C_1 \times \tilde{k}^2$	$C_2 \times \tilde{h}^2$	$C_3 \times \tilde{b}_+^2$	$C_5 \times 2 \tilde{k} \tilde{b}_+$	C_8
$\int \int C_i \times \mathbf{FF}^2$	−61.3	−0.86	−4.43	29.0	0

We notice that the biggest contributions come from the terms where the \tilde{k} form factor appears; that is why we will focus on its determination in the actual lattice computation.

3 Simulation set up

In our analysis we use gauge ensembles produced by European Twisted Mass Collaboration [16–18] with $N_f = 2$ twisted-mass fermions tuned at maximal twist. Parameters of the simulations are collected in Table 2.

The gauge action is tree-level Symanzik improved [21] and reads

$$\begin{aligned} S_G[U] &= \frac{\beta}{6} \left(b_0 \sum_{x, \mu \neq \nu} \text{Tr}(1 - P^{1 \times 1}(x; \mu, \nu)) \right. \\ &\quad \left. + b_1 \sum_{x, \mu \neq \nu} \text{Tr}(1 - P^{1 \times 2}(x; \mu, \nu)) \right), \end{aligned}$$

where $b_0 = 1 - 8b_1$ and $b_1 = -1/12$. The fermionic action with two degenerate flavours is Wilson-like with a twisted-mass term and reads [22–24]:

$$S_F[\chi_q, \bar{\chi}_q, U] = a^4 \sum_x \bar{\chi}_q(x) (D_W + i \mu_q \gamma_5 \tau_3) \chi_q(x),$$

where D_W is the massless Wilson–Dirac operator. In the valence sector we add two doublets of charm quarks and “bottom” quarks. Moreover, as we are interested in computing form factors at different momenta we implement θ -boundary conditions [25], using $\hat{\theta} \equiv (\theta, \theta, \theta)$, for the b doublet:

$$\chi_b(x + L \hat{e}_i) = e^{i\theta L} \cdot \chi_b(x)$$

Table 2 Parameters of the simulations used in this work; masses and momenta are expressed in lattice units. Pion masses are $m_\pi = 420$ MeV for the ensemble ($\beta = 3.9$, $a\mu_{\text{sea}} = 0.0085$) and $m_\pi = 450$ MeV for the ensemble ($\beta = 4.05$, $a\mu_{\text{sea}} = 0.0060$) [19]. The lattice spacing $a_{\beta=3.9}$ is fixed by imposing the matching of f_π obtained on the lattice to the experimental value [19] and $a_{\beta=4.05}$ is rescaled using the parameter $\Lambda_{\overline{\text{MS}}}^{N_f=2}$ [20]. We have added a preliminary use

β	$L^3 \times T$	$a(\text{fm})$	# cnfgs	$\mu_{\text{sea}} = \mu_l$	μ_c	μ_b	$\theta (\pi/L)$
3.9	$24^3 \times 48$	0.085(3)	240	0.0085	0.215	0.3498	0.0, 0.99, 1.41 2.02, 2.50, 2.92 3.66
						0.4839	0.0, 1.21, 1.72 2.46, 3.05, 3.56 4.46
						0.6694	0.0, 1.48, 2.11 3.01, 3.73, 4.36 5.46
						0.3008	0.0, 1.09, 1.56 2.23, 2.76, 3.23 4.04
						0.4162	0.0, 1.35, 1.92 2.74, 3.40, 3.97 4.97
						0.5757	0.0, 1.67, 2.37 3.39, 4.21, 4.91 6.15
4.05	$32^3 \times 64$	0.069(2)	160	0.006	0.1849	0.3008	0.0, 1.09, 1.56 2.23, 2.76, 3.23 4.04
						0.4162	0.0, 1.35, 1.92 2.74, 3.40, 3.97 4.97
						0.5757	0.0, 1.67, 2.37 3.39, 4.21, 4.91 6.15
4.2	$32^3 \times 64$	0.054(2)	300	0.0065	0.1566	0.2548	0.0 0.0 0.0
						0.3525	0.0 0.0 0.0
						0.4876	0.0 0.0 0.0

of data for ($\beta = 4.2$, $a\mu_{\text{sea}} = 0.0065$) and $m_\pi = 495$ MeV. This will be used only for the decay into a scalar charmed meson. The reason is that, with only $\beta = 3.9$ and $\beta = 4.05$, the extrapolation of the decay amplitude $B \rightarrow D_0^* l \nu$ to the physical situation produces a result grieved by more than 100 % error. The data for $\beta = 4.2$, being closer to the continuum, allow for a significant result, as will be seen

This is equivalent to defining the auxiliary field

$$\chi_b^{\bar{\theta}}(x) = e^{-i\bar{\theta} \cdot \vec{x}} \chi_b(x)$$

and the Dirac operator

$$D^{\bar{\theta}}(\chi_b, \bar{\chi}_b, U) \equiv D(\chi_b^{\bar{\theta}}, \bar{\chi}_b^{\bar{\theta}}, U^{\bar{\theta}}) \text{ with } U_i^{\bar{\theta}}(x) = e^{ia\theta} U_i(x).$$

The whole fermionic action finally reads

$$S^{\text{val}} = S_F[\chi_q, \bar{\chi}_q, U] + S_F[\chi_c, \bar{\chi}_c, U] \\ + S_F[\chi_b^{\bar{\theta}}, \bar{\chi}_b^{\bar{\theta}}, U^{\bar{\theta}}].$$

We use all to all propagators with stochastic sources $\eta[i]$ diluted in time [26] and improve the variance-to-signal ratio with the one-end trick [27,28]. When it is generalised to θ -boundary conditions, it consists in solving the Dirac equations,

$$\sum_y D[f, r, \bar{\theta}]_{\alpha\beta}^{ab}(x, y) \phi[i, f, r, \bar{\theta}, \bar{\alpha}, \bar{t}]_{\beta}^b(y) \\ = \eta[i]_{\alpha}^a(x) \delta_{\alpha\bar{\alpha}} \delta_{t_x \bar{t}},$$

where $\tau^3 \chi = r \chi$, f represents the fermion flavour and

$$\sum_y D[f_2, r_2, \bar{\theta}_2]_{\alpha\beta}^{ab}(x, y) \\ \times \Phi[i, f_2, r_2, f_1, r_1, \Gamma_2, \bar{\theta}_2, \bar{\theta}_1, \bar{\alpha}, \bar{t}, \bar{t} + t_S]_{\beta}^b(y) \\ = \Gamma_{2\alpha\beta} \phi[i, f_1, r_1, \bar{\theta}_1, \bar{\alpha}, \bar{t}]_{\beta}^a(x) \delta_{t_S, t_x - \bar{t}}.$$

The stochastic source

$$\xi[i, \bar{\alpha}, \bar{t}]_{\alpha}^a(x) \equiv \eta[i]_{\alpha}^a(x) \delta_{\alpha\bar{\alpha}} \delta_{t_x \bar{t}}$$

is diluted in spinor and is non-zero in a single time slice \bar{t} . It is normalized by

$$\lim_{N \rightarrow \infty} \frac{1}{N} \sum_{i=1}^N \xi[i, \bar{\alpha}, \bar{t}]_{\alpha}^a(x) \xi^*[i, \bar{\alpha}, \bar{t}]_{\beta}^b(y) \\ = \delta_{ab} \delta_{\alpha\beta} \delta_{xy} \delta_{\alpha\bar{\alpha}} \delta_{t_x \bar{t}}.$$

In order to improve the overlap of the interpolating fields for the ground states or to create an operator of higher spin (for instance the tensor meson D_2^*), one has to use interpolating fields, generically written as $\bar{\chi}_1 S \times \Gamma \chi_2$, where S is a path of

links and Γ is any Dirac matrix. We use interpolating fields of the so-called Gaussian smeared form [29]

$$S = \left(\frac{1 + \kappa_G a^2 \Delta}{1 + 6\kappa_G} \right)^R,$$

where $\kappa_G = 0.15$ is a hopping parameter, $R = 30$ is the number of applications of the operator $(1 + \kappa_G a^2 \Delta)/(1 + 6\kappa_G)$ and Δ the gauge-covariant 3D Laplacian constructed from three-times APE-blocked links [30]. If necessary, we also incorporate in S a covariant derivative:

$$\nabla_i \equiv \frac{1}{2a} [U_i(x) - U_i^\dagger(x - \hat{i})].$$

This is relevant to create a tensor meson.

The Dirac equations, which we then have to solve, read

$$\begin{cases} \sum_y D[f, r, \vec{\theta}]_{\alpha\beta}^{ab}(x, y) \phi[i, f, r, S, \vec{\theta}, \vec{\alpha}, \vec{t}]_{\beta}^b(y) = (S \eta[i])_{\alpha}^a(x) \delta_{\alpha\vec{\alpha}} \delta_{t\vec{t}} \\ \sum_y D[f_2, r_2, \vec{\theta}_2]_{\alpha\beta}^{ab}(x, y) \Phi[i, f_2, r_2, f_1, r_1, \Gamma_2, S_2, \vec{\theta}_2, \vec{\theta}_1, \vec{\alpha}, \vec{t}, \vec{t} + t_S]_{\beta}^b(y) \\ = \Gamma_{2\alpha\beta} (S_2 \phi[i, f_1, r_1, \vec{\theta}_1, \vec{\alpha}, \vec{t}])_{\beta}^a(x) \delta_{t_S t_x - \vec{t}}. \end{cases}$$

We compute the “charged” B and D two-point correlators $C_{\vec{\theta}; S_1 \Gamma_1; S_2 \Gamma_2}^{(2)hl}(t)$, which read [32]

$$\begin{aligned} C_{\vec{\theta}; S_1 \Gamma_1; S_2 \Gamma_2}^{(2)hl}(t) &= \frac{1}{2} \sum_{r=\pm 1} \left\langle \text{Tr} \sum_{\vec{x}, \vec{y}} \Gamma_1 \mathcal{S}_l^{S_1}(r; \vec{y}, \vec{t}; \vec{x}, \vec{t} + t) \right. \\ &\quad \times \Gamma_2 \mathcal{S}_h^{S_2}(-r; \vec{x}, \vec{t} + t; \vec{y}, \vec{t}) \Big\rangle, \\ &= \frac{1}{2} \sum_{r=\pm 1} \frac{1}{N} \sum_{n=1}^N \left\langle \text{Tr} \left\{ \sum_{\vec{x}} (\Gamma_1 \gamma_5)_{\vec{\alpha}\vec{\beta}} \phi^*[n, l, r, S_1, \vec{0}, \vec{\beta}, \vec{t}]_{\alpha}^b(\vec{x}, \vec{t} + t) \right. \right. \\ &\quad \times (\gamma_5 \Gamma_2)_{\alpha\beta} (S_2 \phi[n, h, r, \vec{\theta}, \vec{\alpha}, \vec{t}])_{\beta}^b(\vec{x}, \vec{t} + t) \Big\} \Big\rangle, \end{aligned}$$

where $\langle \dots \rangle$ stands for the gauge ensemble average and $h \equiv c$ or b .

We recall that, in twisted-mass QCD, quark propagators have the hermiticity property:

$$\mathcal{S}_q(r; x; y) = \gamma_5 \mathcal{S}_q^\dagger(-r; y; x) \gamma_5.$$

We also compute the “neutral” $B \rightarrow D$ three-point correlators $C_{\vec{\theta}; S_1 \Gamma_1; \Gamma; S_2 \Gamma_2}^{(3)b\Gamma^c}(t, t_S)$, which read

$$\begin{aligned} C_{\vec{\theta}; S_1 \Gamma_1; \Gamma; S_2 \Gamma_2}^{(3)b\Gamma^c}(t, t_S) &= \frac{1}{2} \sum_{r=\pm 1} \left\langle \text{Tr} \sum_{\vec{x}, \vec{y}, \vec{z}} \Gamma \mathcal{S}_c(r, \vec{0}; \vec{z}, \vec{t} + t; \vec{y}, \vec{t}) \Gamma_1 \mathcal{S}_l^{S_1} \right. \\ &\quad \times (-r, \vec{0}; \vec{y}, \vec{t}; \vec{x}, \vec{t} + t_S) \Big\rangle \end{aligned}$$

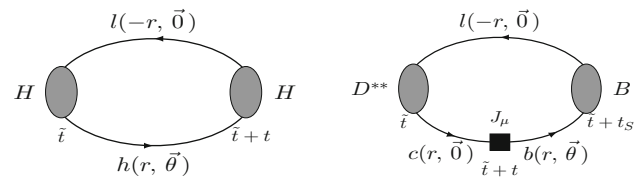


Fig. 1 Kinematical configuration of the two-point correlators (left) and the three-point correlators (right) we compute

$$\begin{aligned} &\times \Gamma_2 \mathcal{S}_b^{S_2}(r, \vec{\theta}; \vec{x}, \vec{t} + t_S; \vec{z}, \vec{t} + t) \Big\rangle, \\ &= \frac{1}{2} \sum_{r=\pm 1} \frac{1}{N} \sum_{n=1}^N \left\langle \text{Tr} \left\{ \sum_{\vec{x}} (\Gamma \gamma_5)_{\vec{\alpha}\vec{\beta}} \right. \right. \\ &\quad \times (\phi[n, c, r, S_1, \vec{0}, \vec{\beta}, \vec{t}])_{\alpha}^b(\vec{x}, \vec{t} + t) \end{aligned}$$

$$\begin{aligned} &\times (\gamma_5 \Gamma_1)_{\alpha\beta} \Phi^*[n, b, -r, l, r, S_2, \Gamma_2, \vec{\theta}, \vec{0}, \vec{\alpha}, \vec{t}, \vec{t} + t_S]_{\beta}^b \\ &\times (\vec{x}, \vec{t} + t) \Big\rangle. \end{aligned}$$

Those two types of correlators are depicted in Fig. 1. On each of the two ensembles, we estimate the statistical error from a jackknife procedure.

4 Masses and energies

We decide to concentrate our effort on the analysis of smeared–smeared two-point correlators because the benefit of such a technique has been already clearly observed in a previous work by ETMC [31]. Masses and energies of pseudoscalar B and D mesons are first extracted from a fit of the form

$$\begin{aligned} C_{PP}(t, \vec{\theta}) &= \frac{\mathcal{Z}^{2(1)}}{2E_P^{(1)}(\vec{\theta})} (e^{-E^{(1)}(\vec{\theta})t} + e^{-E^{(1)}(\vec{\theta})(T-t)}), \\ \mathcal{Z}^{2(1)} &= \langle H^{(1)} O_P^{H\dagger} 0 \rangle \end{aligned}$$

in a time range where the contribution from the first excitation is small compared to the statistical error. The stability of the fit is checked by enlarging the time interval and adding a second exponential in the formula, i.e.,

$$C_{PP}(t, \vec{\theta}) = \sum_{i=1}^2 \frac{\mathcal{Z}^{2(i)}}{2E_P^{(i)}(\vec{\theta})} (e^{-E^{(i)}(\vec{\theta})t} + e^{-E^{(i)}(\vec{\theta})(T-t)}).$$

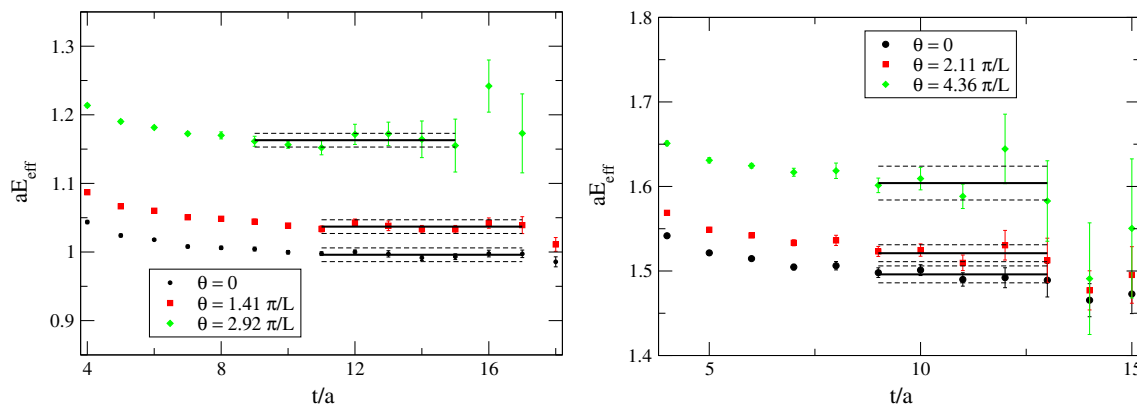


Fig. 2 Effective energies of “ B ”-mesons measured with the ETMC ensemble ($\beta = 3.9$, $\mu_{\text{sea}} = \mu_l = 0.0085$): $\mu_h = 0.3498$ (left) and $\mu_h = 0.6694$ (right)

The last step in the analysis is to measure the effective energy $E_P \equiv E_P^{(1)}$ of the ground state from the ratio

$$\frac{C_{PP}(t+1, \vec{\theta})}{C_{PP}(t, \vec{\theta})} = \cosh(E_P(\vec{\theta})) + \sinh(E_P(\vec{\theta})) \tanh[E_P(\vec{\theta})(t - T/2)].$$

We show in Fig. 2 examples of plateaus for “ B ”-mesons energies at three different momenta.

We study the dispersion relation to get an idea of the magnitude of cut-off effects. We display in Fig. 3 the B meson energies and compare them to the theoretical formula

$$\sinh^2[aE(\theta)/2] = \sinh^2[aM/2] + 3 \sin^2(\theta/2) \quad \text{where } M \equiv E(0). \quad (4.1)$$

The agreement is good at the two lightest heavy masses but really bad at the heaviest one: cut-off effects are pretty large.

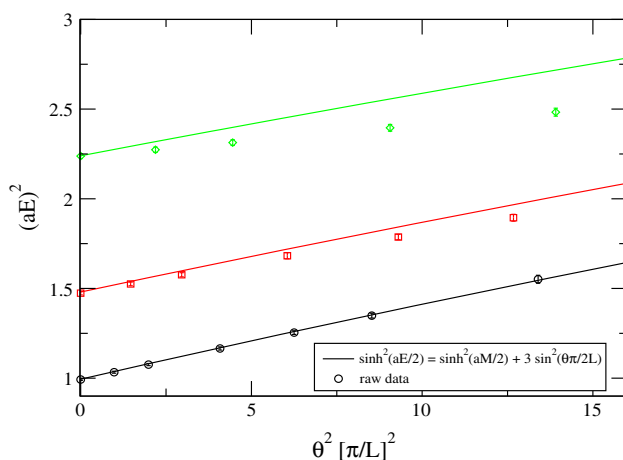


Fig. 3 Comparison of the “ B ”-mesons energies with the dispersion relation, at the ETMC ensemble ($\beta = 3.9$, $\mu_{\text{sea}} = \mu_l = 0.0085$). The energy has been rescaled to 1 for the lightest B at rest. The black, red and green points correspond to the three B masses in increasing order

Interpolating fields of the 2^+ state are given by the formula $O^{(\lambda)} = \epsilon_{\mu\nu}^{*(\lambda)} \bar{\chi}_c \gamma_\mu \nabla_\nu \chi_l$, $\lambda = \pm 2, \pm 1, 0$. Actually we choose to use linear combinations of the interpolating fields that read

$$\begin{cases} \tilde{O}^{(1)} = \frac{1}{\sqrt{2}}(O^{(+2)} + O^{(-2)}) = \frac{1}{\sqrt{2}} \bar{\chi}_c (\gamma_1 \nabla_1 - \gamma_2 \nabla_2) \chi_l \\ \tilde{O}^{(2)} = O^{(0)} = -\frac{1}{\sqrt{6}} \bar{\chi}_c (\gamma_1 \nabla_1 + \gamma_2 \nabla_2 - 2\gamma_3 \nabla_3) \chi_l \\ \tilde{O}^{(3)} = \frac{1}{\sqrt{2}}(O^{(+2)} - O^{(-2)}) = -\frac{i}{\sqrt{2}} \bar{\chi}_c (\gamma_1 \nabla_2 + \gamma_2 \nabla_1) \chi_l \\ \tilde{O}^{(4)} = \frac{1}{\sqrt{2}}(O^{(+1)} + O^{(-1)}) = \frac{i}{\sqrt{2}} \bar{\chi}_c (\gamma_2 \nabla_3 + \gamma_3 \nabla_2) \chi_l \\ \tilde{O}^{(5)} = \frac{1}{\sqrt{2}}(O^{(+1)} - O^{(-1)}) = -\frac{i}{\sqrt{2}} \bar{\chi}_c (\gamma_1 \nabla_3 + \gamma_3 \nabla_1) \chi_l. \end{cases}$$

The two first interpolating fields live in the E representation of the O_h cubic group symmetry of rotations and inversion in a 3D spatial lattice, while the last three live in the T_2 representation of that group [33]. We finally consider the r -symmetrized smeared-smeared two-point correlators

$$C_{2^+, E}^{(2)}(t) = \frac{1}{2} \left[\left\langle \sum_{\vec{x}, \vec{y}} \tilde{O}_S^{(1)}(\vec{y}, t + \tilde{t}) \tilde{O}_S^{\dagger(1)}(\vec{x}, \tilde{t}) \right\rangle + \left\langle \sum_{\vec{x}, \vec{y}} \tilde{O}_S^{(2)}(\vec{y}, t + \tilde{t}) \tilde{O}_S^{\dagger(2)}(\vec{x}, \tilde{t}) \right\rangle \right] \quad (4.2)$$

and

$$C_{2^+, T_2}^{(2)}(t) = \frac{1}{3} \left[\left\langle \sum_{\vec{x}, \vec{y}} \tilde{O}_S^{(3)}(\vec{y}, t + \tilde{t}) \tilde{O}_S^{\dagger(3)}(\vec{x}, \tilde{t}) \right\rangle + \left\langle \sum_{\vec{x}, \vec{y}} \tilde{O}_S^{(4)}(\vec{y}, t + \tilde{t}) \tilde{O}_S^{\dagger(4)}(\vec{x}, \tilde{t}) + \left\langle \sum_{\vec{x}, \vec{y}} \tilde{O}_S^{(5)}(\vec{y}, t + \tilde{t}) \tilde{O}_S^{\dagger(5)}(\vec{x}, \tilde{t}) \right\rangle \right]. \quad (4.3)$$

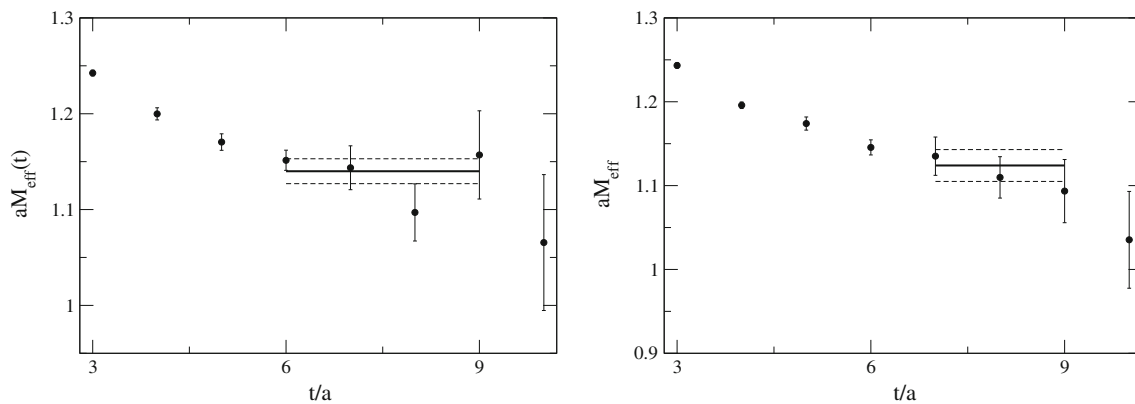


Fig. 4 Effective mass of the D_2^* meson measured with the ETMC ensemble ($\beta = 3.9$, $\mu_{\text{sea}} = \mu_l = 0.0085$): $\frac{C_{2+,E}^{(2)}(t)}{C_{2+,E}^{(2)}(t+1)}$ (left) and $\frac{C_{2+,T_2}^{(2)}(t)}{C_{2+,T_2}^{(2)}(t+1)}$ (right)

The masses we extract by studying the ratios $\frac{C_{2+,E}^{(2)}(t)}{C_{2+,E}^{(2)}(t+1)}$ and $\frac{C_{2+,T_2}^{(2)}(t)}{C_{2+,T_2}^{(2)}(t+1)}$ are in principle equal: any discrepancy comes from cut-off effects. We show in Fig. 4 that, indeed, lattice artefacts are present.

As parity is broken by the twisted-mass action at finite lattice spacing [23] and the states we consider are not made with quarks of the same flavour doublet, contrary to what is discussed in Sect. 5.2 of [24], the scalar D meson can in principle mix with the pseudoscalar D meson. We have to build a matrix of correlators $\{C_{ij}(t)\}$ and solve a generalised eigenvalue problem (GEVP) [34–36]. We study a 2×2 system whose entries correspond to the interpolating fields with Dirac structures $\bar{\chi}_c \gamma^5 \chi_l$ and $\bar{\chi}_c \chi_l$:

$$C_{ij}(t) = \begin{bmatrix} C_{\bar{\chi}_c \gamma^5 \chi_l; \bar{\chi}_l \gamma^5 \chi_c}^{(2)}(t) & C_{\bar{\chi}_c \gamma^5 \chi_l; i \bar{\chi}_l \chi_c}^{(2)}(t) \\ C_{-i \bar{\chi}_c \chi_l; \bar{\chi}_l \gamma^5 \chi_c}^{(2)}(t) & C_{\bar{\chi}_c \chi_l; \bar{\chi}_l \chi_c}^{(2)}(t) \end{bmatrix}.$$

We solve the system

$$C_{ij}(t) v_j^{(n)}(t, t_0) = \lambda^{(n)}(t, t_0) C_{ij}(t_0) v_j^{(n)}(t, t_0). \quad (4.4)$$

We set $t_0 = 3$ ($\beta = 3.9$) and 5 ($\beta = 4.05$). $\lambda^{(n)}(t, t_0)$ and $v^{(n)}(t, t_0)$ are the eigenvalues and eigenvectors of the matrix $C^{-1}(t_0)C(t)$. The effective mass $m_{D_0^*}$ of the scalar meson is given by

$$\lambda^{(2)}(t, t_0) = \frac{\cosh[m_{D_0^*}(T/2 - t)]}{\cosh[m_{D_0^*}(T/2 - t_0)]} \quad (4.5)$$

We show in Fig. 5 $m_{D_0^*}$ for the ensemble ($\beta = 3.9$, $\mu_{\text{sea}} = 0.0085$). The signal is unfortunately quite short, but still acceptable for our qualitative study.

We collect in the “Appendix” all the masses and energies that we extracted in our analysis. The total error includes the statistical one and the discrepancy of results when we change the time range $[t_{\min}, t_{\max}]$ of the fits by $t_{\min} \pm 1$ and

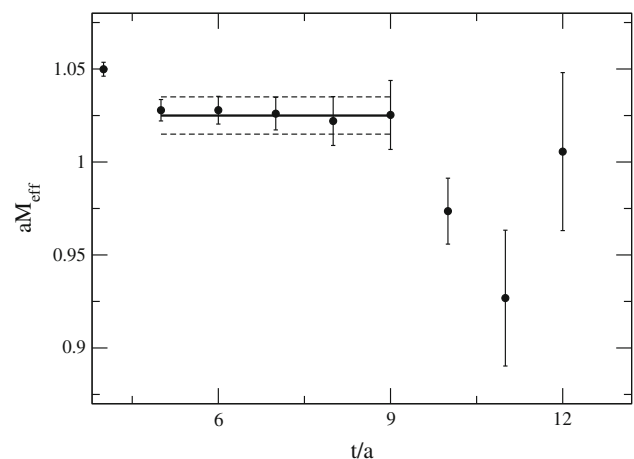


Fig. 5 Effective mass of the D_0^* meson measured with the ETMC ensemble ($\beta = 3.9$, $\mu_{\text{sea}} = \mu_l = 0.0085$)

$t_{\max} \pm 1$, when we take different t_0 in the range $[3, 6]$ and, in the case of pseudoscalar B mesons, when we perform a two-state exponential fit.

4.1 $M_{D_2^*} - M_D$ and $M_{D_0^*} - M_D$ in the continuum limit and experiment

In Table 7 in the “Appendix” are given the masses of the D_2^* , D_0^* and D mesons. It is interesting to perform an extrapolation to the continuum and compare with the experimental data. For the latter we will take the $c\bar{s}$ mesons. It does not change anything for the tensor meson as compared to the non-strange charmed mesons ($M_{D_2^*}(2460) - M_D \simeq M_{D_{2s}^*}(2573) - M_{D_s}$) but for the scalar mesons it does, since the $D_{0s}^*(2317)$ has a narrow and clear signal which is not the case of the $D_0^*(2400)$ whose signal is very broad due to its S-wave decay into $D\pi$.

We perform the extrapolation to the continuum limit and compute the error using jackknife. We show our results in

Table 3 Mass differences $M_{D_0^*} - M_D$ (third column) and $M_{D_2^*} - M_D$ (fourth column) for $\beta = 3.9$ (first line), $\beta = 4.05$ (second line) and $\beta = 4.2$ (third line), the latter being for the moment restricted to $M_{D_0^*} - M_D$. We use the lattice spacings reported in Table 2. The extrapolation to vanishing lattice spacing is in the fourth line and the experimental data $M_{D_0^*}(2317) - M_{D_s}$ and $M_{D_2^*}(2573) - M_{D_s}$ are in the fifth line. The errors combine in quadrature the errors on the masses in lattice units and on the lattice spacing. The fitting windows are reported in Table 7. The dependence of the value extrapolated to continuum strongly depends on the lattice spacing. Our uncertainty does not incorporate the systematic one due to the choice of the fitting windows. Our mass differences extrapolated to the continuum are above experiment

Lattice spacing (fm)	Inverse spacing (GeV)	Scalar	Tensor
0.085 (3)	2.32 (8)	0.58 (9)	0.88 (7)
0.069 (2)	2.85 (8)	0.51 (5)	0.88 (5)
0.0054 (2)	3.65 (8)	0.51 (5)	
0.0	Inf	0.44 (7)	0.88 (7) $\left(\begin{smallmatrix} +15 \\ -18 \end{smallmatrix}\right)$
Exp.		0.349	0.605

Table 3. We see that the agreement with experiment is not so good but the errors are large. For the moment we cannot say much, except that the future will tell whether this issue comes mainly from statistical fluctuations or whether the lattice regularisation is in cause. A similar conclusion was drawn recently in a lattice study with $N_f = 2 + 1 + 1$ dynamical quarks regularised by TmQCD [39]. Also, we have not considered yet the possible effect of the opening of the decay channel $D_0^* \rightarrow D\pi$ S-wave state as proposed in [40].

5 B decay to the scalar D_0^* charmed meson

In this section we will restrict our treatment to the zero recoil kinematics, in other words, the initial B meson is taken at rest. We restrict ourselves to this simpler case because the momentum dependence of the $B \rightarrow D_0^*$ decay is very difficult to study on the lattice (three-point correlators are very noisy) and we cannot yet say anything significant about it, but also because the non-vanishing of the zero recoil amplitude is of utmost phenomenological relevance: in the infinite mass limit, the $B \rightarrow D_0^*$ amplitude vanishes at zero recoil [13]. This forbids the decay into an S-wave between the lepton pair and the D_0^* , since an S-wave clearly does not vanish at zero recoil. The S-wave is a major contribution to these decays, since their available phase space is rather small, and higher waves are suppressed by the so-called centrifugal barrier effect. With finite heavy quark masses we will show that the zero recoil amplitude *does not vanish*, there is a non-vanishing S-wave and this may change drastically the ratio between $\Gamma(B \rightarrow D_2^*)$ and $\Gamma(B \rightarrow D_0^*)$, since the $B \rightarrow D_2^*$ decay amplitude does vanish at zero recoil whether the mass of the c and b is taken infinite or finite, thus implying only D-wave decay. The possible importance of a non-vanishing

zero recoil amplitude was stressed in [37], where the authors estimated subleading corrections to the infinite mass limit: although subleading in the $\Lambda/m_{c,b}$ expansion, the S-wave may not be negligible. Our computation confirms this conclusion as shall be seen.

5.1 Computation of the amplitude ratio ($B \rightarrow D_0^*$) over ($B \rightarrow D$) at zero recoil

We will compute the ratio of the amplitudes $A(B \rightarrow D_0^*)/A(B \rightarrow D)$. We take $A(B \rightarrow D)$ as a benchmark, since it is experimentally fairly well known, and D being a $J = 0$ state as D_0^* , it is expected that the momentum dependence of these decays will be rather similar. We recall some formulae neglecting for the moment the D – D_0^* mixing due to the parity violation at finite lattice spacing when using twisted-mass quarks. The matrix elements $\langle B|V_0|D \rangle$ and $\langle B|A_0|D_0^* \rangle$ are given by the following ratio:

$$\langle B|O|H_c \rangle = \frac{C_{\text{BOH}_c}^{(3)}(t_p, t, t_s) \sqrt{Z_{H_c}/Z_B} Z_O}{C_{H_c}^{(2)}(t - t_s) \exp(-E_B(t_p - t)) / (2E_B)}, \quad (5.1)$$

where $t_s < t < t_p$ are, respectively, the source, current and sink times (cf. Fig. 1).

$Z_0 = Z_V(Z_A)$ when $H_c = D(D_0^*)$. Z_{H_c} and Z_B are defined from the fit of the two-point correlators of the H_c and B mesons, assuming we are far enough from the centre of the lattice to be allowed to neglect the backward exponential in time while the contribution of excited states is small:

$$C_B^{(2)}(t, \vec{\theta}) = \frac{Z_B}{2E_B(\vec{\theta})} \exp(-E_B(\vec{\theta})t);$$

$$C_{H_c}^{(2)}(t, 0) = \frac{Z_{H_c}}{2M_{H_c}} \exp(-M_{H_c}t). \quad (5.2)$$

Then we compute

$$\frac{\langle B|A_0|D_0^* \rangle}{\langle B|V_0|D \rangle} = \frac{C_{\text{BA}_0D_0^*}^{(3)}(t_p, t, t_s) C_D^{(2)}(t - t_s) Z_A \sqrt{Z_{D_0^*}}}{C_{\text{BV}_0D}^{(3)}(t_p, t, t_s) C_{D_0^*}^{(2)}(t - t_s) Z_V \sqrt{Z_D}}. \quad (5.3)$$

5.2 Taking into account the scalar–pseudoscalar mixing

In Sect. 4 we have detailed the generalised eigenvalue method. As explained there and in Sect. 3, we restrict ourselves to a 2×2 matrix of smeared and stochastic two-point correlators. The largest (smallest) eigenvalue $\lambda^{(1)}$ ($\lambda^{(2)}$) will be related to the mass of the D (D_0^*) state. The corresponding eigenvectors give the linear combination of $\bar{\chi}_c \gamma_5 \chi_l$ and $\bar{\chi}_c \chi_l$ interpolating fields that have the largest coupling to the $D(D_0^*)$ state. The eigenvectors turn out to be not far from orthogonal

Table 4 Values of the approximately orthonormalised eigenvectors $v^{(1)}$ and $v^{(2)}$, Eq. (4.5), for $\beta = 3.9$, $t_0 = t_s = 3$, $t = 7$ and $t_p = 14$. $v^{(1)}v^{(2)\dagger} = 0.07i$, rather small as expected in Eq. (5.4)

$v^{(1)}$	$v^{(2)}$
0.97	0.28i
0.22i	0.96

$$v^{(1)}v^{(2)\dagger} = \sum_{k=1,2} v_k^{(1)}v_k^{(2)*} = 0.07i \simeq 0, \quad (5.4)$$

as seen for example in Table 4. One might say that 0.07 is not so small but this is not surprising, since there are other states in which the B might decay than only the ground state scalar and pseudoscalar that we consider in our analysis. We can thus to a fair approximation orthonormalise the eigenvectors so that

$$v^{(i)}v^{(j)\dagger} \simeq \delta_{i,j}, \quad (5.5)$$

without changing the eigenvalues, since in Eq. (4.4) the same factor multiplies both sides of the equation. Thus, we define the two-point correlator of the D_0^* meson by

$$\begin{aligned} \lambda^{(2)}(t-t_s, t_0) &= \sum_{i,j=1}^2 v_i^{(2)\dagger}(t-t_s, t_0) C_{ij}^{(2)}(t_0) v_j^{(2)}(t-t_s, t_0) \\ &= \sum_{i,j=1}^2 v_i^{(2)\dagger}(t-t_s, t_0) C_{ij}^{(2)}(t-t_s) v_j^{(2)}(t-t_s, t_0), \\ \lambda^{(1)}(t-t_s, t_0) &= \sum_{i,j=1}^2 v_i^{(1)\dagger}(t-t_s, t_0) C_{ij}^{(2)}(t_0) v_j^{(1)}(t-t_s, t_0) \\ &= \sum_{i,j=1}^2 v_i^{(1)\dagger}(t-t_s, t_0) C_{ij}^{(2)}(t-t_s) v_j^{(1)}(t-t_s, t_0), \end{aligned} \quad (5.6)$$

where we fit with

$$\begin{aligned} \lambda^{(2)}(t-t_s, t_0) &= \exp(-M_{D_0^*}(t-t_s-t_0)) \\ \lambda^{(1)}(t-t_s, t_0) &= \exp(-M_D(t-t_s-t_0)), \end{aligned} \quad (5.7)$$

since $\lambda^{(i)}(t_0, t_0) = 1$ from Eq. (5.6). We define $Z_2^{(1)}$ and $Z_2^{(2)}$ from

$$\begin{aligned} v_i^{(2)\dagger}(t-t_s, t_0) C_{ij}^{(2)}(t-t_s) v_j^{(2)}(t-t_s, t_0) &= \frac{Z_2^{(2)}}{2M_{D_0^*}} \exp(-M_{D_0^*}(t-t_s)), \\ v_i^{(1)\dagger}(t-t_s, t_0) C_{ij}^{(2)}(t-t_s) v_j^{(1)}(t-t_s, t_0) &= \frac{Z_1^{(1)}}{2M_{D_0^*}} \exp(-M_D(t-t_s)). \end{aligned} \quad (5.8)$$

In Eq. (5.1) we see that the factors Z_i appear only via their square root.

5.2.1 Symmetry properties of the matrix elements

In the continuum it is obvious by parity conservation that

$$\langle B|A_0|D \rangle = \langle B|V_0|D_0^* \rangle = 0. \quad (5.9)$$

However, parity is not conserved by the twisted-mass quark action at finite lattice spacing. But this action has an exact symmetry [23], the flavour-parity

$$\mathcal{R}_5^{\text{sp}} \equiv \mathcal{P} \otimes (\mu_l, \mu_c, \mu_b \rightsquigarrow -\mu_l, -\mu_c, -\mu_b) \quad (5.10)$$

where \mathcal{P} is the spatial parity, and μ_l, μ_c, μ_b are the twisted-mass terms for the light, charm and beauty quarks. We assume we are at maximal twist (vanishing of m_{PCAC}). Therefore if we use

$$C_{i,j,k}^{(3)\text{sym}}(t_p, t, t_s) \equiv (1 + \mathcal{R}_5^{\text{sp}}) C_{i,j,k}^{(3)}(t_p, t, t_s), \quad (5.11)$$

we get the validity of Eq. (5.9) also for finite lattice spacing. This symmetrisation will be assumed in the following.

5.2.2 GEVP on the three-point correlators

In this section we assume $t_s < t < t_p$ and $t_0 \leq t - t_s$. Starting from the three-point correlators $C_{BA_0(V_0)O_i}^{(3)}(t_p, t, t_s) = \langle \bar{\chi}_b \gamma_5 \chi_l(t_p) A_0(V_0)(t) O_i(\bar{\chi}_c, \chi_l, t_s) \rangle$, $O_i(\bar{\chi}_c, \chi_l) \equiv \{\bar{\chi}_c \gamma_5 \chi_l, \bar{\chi}_c \chi_l\}$ and following the authors [38] as regards their way of extracting the decay constant f_B , we consider the projected three-point correlators

$$\begin{aligned} C_{BA_0D_0^*}^{(3)'}(t_p, t, t_s) &= \frac{\langle \bar{\chi}_b \gamma_5 \chi_l(t_p) A_0(t) \bar{\chi}_c \chi_l(t_s) v_{\bar{\chi}_c \chi_l}^{(2)}(t-t_s, t_0) \rangle}{\sqrt{v_i^{\dagger(2)}(t-t_s, t_0) C_{ij}^{(2)}(t-t_s) v_j^{(2)}(t-t_s, t_0)}} \\ &\quad \times \left(\frac{\lambda^{(2)}(t_0+a, t_0)}{\lambda^{(2)}(t_0+2a, t_0)} \right)^{(t-t_s)/2a} \frac{2E_B e^{(t_p-t)E_B}}{\sqrt{Z_B}} \sqrt{2m_{D_0^*}}, \\ C_{BV_0D}^{(3)'}(t_p, t, t_s) &= \frac{\langle \bar{\chi}_b \gamma_5 \chi_l(t_p) V_0(t) \bar{\chi}_c \gamma_5 \chi_l(t_s) v_{\bar{\chi}_c \gamma_5 \chi_l}^{(1)}(t-t_s, t_0) \rangle}{\sqrt{v_i^{\dagger(1)}(t-t_s, t_0) C_{ij}^{(2)}(t-t_s) v_j^{(1)}(t-t_s, t_0)}} \\ &\quad \times \left(\frac{\lambda^{(1)}(t_0+a, t_0)}{\lambda^{(1)}(t_0+2a, t_0)} \right)^{(t-t_s)/2a} \frac{2E_B e^{(t_p-t)E_B}}{\sqrt{Z_B}} \sqrt{2m_D}. \end{aligned} \quad (5.12)$$

We recall that the normalisation factor $Z_2^{(2)}$ cancels between $\langle \bar{\chi}_b \gamma_5 \chi_l(t_p) A_0(V_0)(t) \bar{\chi}_c \gamma_5 \chi_l(t_s) \rangle$ and $\sqrt{v_i^{\dagger(2(1))}(t-t_s, t_0) C_{ij}^{(2)}(t-t_s) v_j^{(2(1))}(t-t_s, t_0)}$ while the factor $\left(\frac{\lambda^{(2(1))}(t_0+a, t_0)}{\lambda^{(2(1))}(t_0+2a, t_0)} \right)^{(t-t_s)/2a} \sim e^{-E_{D_0^*(D)}(t-t_s)/2a}$ compensates the residual time exponential dependence. We do not take into account the contributions $\propto v_{\bar{\chi}_c \gamma_5 \chi_l}^{(2)}(t-t_s, t_0)$ and $v_{\bar{\chi}_c \chi_l}^{(1)}(t-t_s, t_0)$ to the projected correlators

Table 5 We give the ratios defined in Eq. (5.13) over a plateau corresponding to [6–10] in units of lattice spacing for $\beta = 4.2$. The lattice points at the other β 's do not match with those at $\beta = 4.2$. To explain our method, let us take a point $x_{4.2}$, we take for $\beta = 3.9$ the two points $y_{3.9}$ and $y_{3.9} + 1$ such that $y_{3.9} * a_{3.9}/a_{4.2} < x_{4.2} < (y_{3.9} + 1)a_{3.9}/a_{4.2}$. Then from any function f computed for 3.9 we define the interpolated function $f_{\text{res}} = f(y_{3.9})((y_{3.9} + 1)a_{3.9}/a_{4.2} - x_{4.2}) + f(y_{3.9} + 1)(x_{4.2} - y_{3.9}a_{3.9}/a_{4.2})$. The b quarks range from the lightest to heaviest from left to right: $m_B \simeq 2.55, 3.18, 3.97$ GeV. The right column corresponds to the extrapolation at the physical B mass: 5.2 GeV. The last line corresponds to the extrapolation to the continuum. The errors are only statistical except on the physical case (bottom-right) where the second error takes into account a systematic error estimated from the dependence of our result on the window choices to compute the masses and on the method in extrapolating to the physical point (in $1/m_B$ or in $1/\mu_b^{MS}(2\text{GeV})$)

β	Ratio $m_{b(1)}$	Ratio $m_{b(2)}$	Ratio $m_{b(3)}$	Ratio at physical B
3.9	0.23 (3)	0.17 (2)	0.11 (3)	0.06 (4)
4.05	0.20 (2)	0.14 (2)	0.08 (4)	0.03 (5)
4.2	0.23 (2)	0.19 (3)	0.17 (3)	0.14 (4)
Continuum	0.22 (5)	0.17 (5)	0.17 (7)	0.17(6)(6)

$\sum_i \langle \bar{\chi}_b \gamma_5 \chi_l(t_p) A_0(V_0)(t) O_i(\bar{\chi}_c, \chi_l, t_s) v_i^{(2(1))}(t - t_s, t_0) \rangle$ because the B meson goes through operator $A_0(V_0)$ only to a pure scalar (pseudoscalar) state.

The ratio in Eq. (5.3) becomes

$$\frac{\langle B|A_0|D_0^* \rangle}{\langle B|V_0|D \rangle} \simeq \frac{C_{\text{BA}_0D_0^*}^{(3')}(t_p, t, t_s)}{C_{\text{BV}_0D}^{(3')}(t_p, t, t_s)} \times \frac{Z_A}{Z_V} \quad (5.13)$$

using Eq. (5.7)

Of course the ratio of branching fractions has to take into account the difference in phase space. However, we ignore totally the dependence of the amplitude on the recoil, having only estimated the zero recoil contribution. Therefore, we will for the moment neglect the phase space dependence. We collect the results of Eq. (5.13) in Table 5 and show plateaus in Fig. 6.

The values of the plateaus are reported in Table 5. The dependence in m_B agrees with the formula $c/m_B + b$. We show both the extrapolation to the physical B meson and the vanishing lattice spacing. When both extrapolations are combined we get a ratio of 0.17(6)(6). This is a non-vanishing signal, thanks to the data at $\beta = 4.2$, which, lying closer to the continuum, constrain more efficiently the continuum limit.

As a gross estimate the ratio of branching fractions is the square of the ratio of amplitudes reported in Table 5. The experimental value of the ratios of branching fractions can be very grossly estimated to be around 0.1–0.2, which would correspond to a ratio of amplitudes ~ 0.3 –0.45. Our estimate lies below this value, but at this stage we must remain very careful: the experimental status of the D_0^* is unclear, the

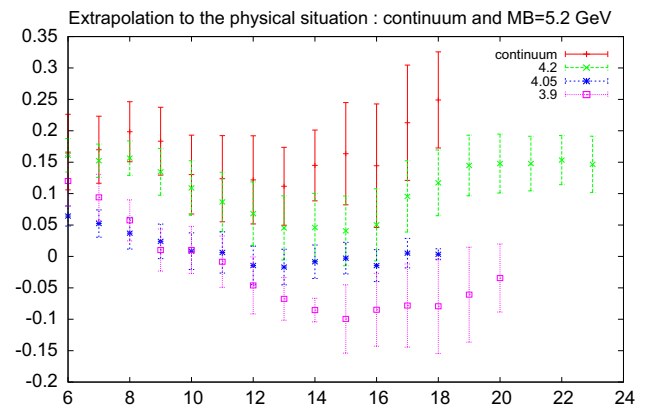


Fig. 6 The ratio in Eq. (5.13) once symmetrised according to Eq. (5.11) extrapolated from the three b quark masses to the physical B mass: 5.2 GeV, linearly in $1/M_B$. We have used data from $\beta = 3.9, 4.05, 4.2$. The time unit is the lattice spacing for $\beta = 4.2$: $a \simeq 0.054$ fm. The ratios for $\beta = 3.9, 4.05$ have been interpolated to points in $a_{\beta=4.2}$ lattice units using the formula which is detailed in the caption of Table 5. The plot starts at $t = 6$, the time t_0 of the GEVP procedure. We see acceptable plateaus up to $t = 10$ and we compute the averages to be between 6 and 10, as reported in Table 5. For larger times the signal falls down, presumably because of the parity violation when using twisted masses which induces the scalar D_0^* to “decay” into the pseudoscalar D meson. The error bars are only statistical errors

resonance being very broad, and our theoretical estimate is affected by very large uncertainties. Also the experimental situation is far from clear for the moment [4].

6 B decay to the tensor ($J = 2^+$) charmed meson

In this section we want to estimate the amplitudes for $B \rightarrow D_2^* \ell \nu$ decay. In [1] the spin-2 charmed mesons are named $D_2^*(2460)$ ($D_{s2}^*(2573)$). For the initial B meson, we use three “ B_i , $i = 1, 2, 3$ ” with increasing masses valued 2.55, 3.18 and 3.97 GeV. As was mentioned before, the “ B_i , $i = 1, 2, 3$ ” are moving while the final charmed meson is at rest. We concentrate on the calculation of the form factor \tilde{k} , since it was shown in Sect. 2.5 that it is, by large, dominant in the decay width.

6.1 Three-point correlators computed for $B \rightarrow D(2^+)$

We start from the formulae recalled in Sect. 2.5. We use a symbolic notation to represent the hadronic matrix elements

$$H_{i,j,k} = \langle B|A_k|D_2^*(\epsilon_{ij}^{(\lambda)}) \rangle \rightsquigarrow A_k V_j D_i.$$

The various combinations to extract \tilde{k} are collected in Table 6. We consider all of these combinations and average the resulting value for \tilde{k} . To eliminate artefacts we must also apply the symmetrized result according to Eq. (5.11)

Table 6 Combinations of three-point correlators used to extract \tilde{k}

Combination	Expression
$p\tilde{k} = -\sqrt{6}\mathcal{T}_{1(0)}^A$	$A_1 V_1 D_1 + A_1 V_2 D_2 - 2 A_1 V_3 D_3$
$p\tilde{k} = -\sqrt{6}\mathcal{T}_{2(0)}^A$	$A_2 V_1 D_1 + A_2 V_2 D_2 - 2 A_2 V_3 D_3$
$p\tilde{k} = \sqrt{6}/2 \mathcal{T}_{3(0)}^A$	$-(A_3 V_1 D_1 + A_3 V_2 D_2 - 2 A_3 V_3 D_3)/2$
$p\tilde{k} = [\mathcal{T}_{1(+2)}^A + \mathcal{T}_{1(-2)}^A]$	$(A_1 V_1 D_1 - A_1 V_2 D_2)/2$
$p\tilde{k} = -[\mathcal{T}_{2(+2)}^A + \mathcal{T}_{2(-2)}^A]$	$-(A_2 V_1 D_1 - A_2 V_2 D_2)/2$
$p\tilde{k} = i\{[\mathcal{T}_{1(+2)}^A - \mathcal{T}_{1(-2)}^A] + [\mathcal{T}_{1(+1)}^A + \mathcal{T}_{1(-1)}^A]\}$	$A_1 V_1 D_2 + A_1 V_2 D_1 - A_1 V_3 D_2 - A_1 V_2 D_3$
$p\tilde{k} = -i\{[\mathcal{T}_{3(+2)}^A - \mathcal{T}_{3(-2)}^A] + [\mathcal{T}_{3(+1)}^A + \mathcal{T}_{3(-1)}^A]\}$	$-A_3 V_1 D_2 - A_3 V_2 D_1 + A_3 V_3 D_2 + A_3 V_2 D_3$
$p\tilde{k} = i\{[\mathcal{T}_{1(+1)}^A + \mathcal{T}_{1(-1)}^A] + i[\mathcal{T}_{1(+1)}^A - \mathcal{T}_{1(-1)}^A]\}$	$A_1 V_1 D_3 + A_1 V_3 D_1 - A_1 V_3 D_2 - A_1 V_2 D_3$
$p\tilde{k} = -i\{[\mathcal{T}_{2(+1)}^A + \mathcal{T}_{2(-1)}^A] + i[\mathcal{T}_{2(+1)}^A - \mathcal{T}_{2(-1)}^A]\}$	$-A_2 V_1 D_3 - A_2 V_3 D_1 + A_2 V_3 D_2 + A_2 V_2 D_3$
$p\tilde{k} = i\{[\mathcal{T}_{2(+2)}^A - \mathcal{T}_{2(-2)}^A] + i[\mathcal{T}_{2(+1)}^A - \mathcal{T}_{2(-1)}^A]\}$	$A_2 V_1 D_2 + A_2 V_2 D_1 - A_2 V_3 D_1 - A_2 V_1 D_3$
$p\tilde{k} = -i\{[\mathcal{T}_{3(+2)}^A - \mathcal{T}_{3(-2)}^A] - i[\mathcal{T}_{3(+1)}^A - \mathcal{T}_{3(-1)}^A]\}$	$-A_3 V_1 D_2 - A_3 V_2 D_1 + A_3 V_3 D_1 + A_3 V_1 D_3$

6.2 Subtracting zero momentum three-point correlators

The three-point correlation functions involving a tensor D meson are unfortunately very noisy: hence it is extremely difficult to get a large enough signal-to-noise ratio. We will use a trick³ which consists in subtracting to every three-point correlator the correlator with the same gauge configuration and the same operators at zero momentum. Indeed we know that the decay $B \rightarrow D_2^*$ vanishes at zero recoil. This is obvious in the continuum limit, since we start with a B meson of vanishing angular momentum J . The weak interaction operator (axial current A_μ), having $J = 0$ for A_0 and $J = 1$ for A_i ($i = 1, 2, 3$), cannot generate a $J = 2$ state: at zero recoil there is no momentum to generate a higher angular momentum.

However, this vanishing is also exact on a lattice. The proof goes as follows: the three-point correlators which contribute to the $D_2^* \rightarrow B$ are linear combinations of correlators of the type

$$C_{i,j,k}^{(3)}(t_p, t, t_s) = \langle O_B(t_p) A_k(t) O_{D_i} V_j(t_s) \rangle, \quad (6.1)$$

where $i, j, k \in \{1, 2, 3\}$ may be different or equal. All operators are at rest (zero recoil). We have assumed the D_2^* meson (B meson) interpolating field to be at the source time t_s (sink time t_p), and the current at time t with $t_p \geq t \geq t_s$.

Let us choose one of the three spatial directions \hat{l} and consider the rotation $\mathcal{R}_l(\pi)$ of angle π around it: the spatial coordinates perpendicular to \hat{l} change sign. All vector operators, D_i , V_i and A_i , change sign if i is perpendicular to \hat{l} , whereas they remain unchanged if $i = l$.

$\mathcal{R}_l(\pi)$ belongs to the 3D cubic symmetry group. The lattice actions are invariant under $\mathcal{R}_l(\pi)$, even the twisted-mass action since $\mathcal{R}_l(\pi)$ is parity even. In Eq. (6.1), there are

three operators at three different times. Being at rest, we may assume that their spatial nesting is invariant under $\mathcal{R}_l(\pi)$: it can be a stochastic source, a local operator at the origin of three-space, a smeared operator symmetric around the origin of three-space or a local operator integrated over three-space (for the current). If an odd number among the indices i, j, k are perpendicular to \hat{l} , then the correlator in Eq. (6.1) changes sign under $\mathcal{R}_l(\pi)$ and the amplitude must vanish. This happens if $i = j = k, \hat{l}$ being any other direction, or if $i = j \neq k, l = i$.

However, if i, j, k are all different it does not work: any $\mathcal{R}_l(\pi)$ will keep the $C^{(3)}$ of Eq. (6.1) unchanged and thus cannot be proven to vanish on the lattice although it should in the continuum limit. This type of term does generate lattice artefacts. A parity operation would change its sign (changing the sign of all three operators) but parity is not an invariant of the twisted-mass action. We must then use correlators symmetrised according to the exact symmetry of the twisted-mass action [23], i.e. we apply Eq. (5.11): the lattice artefact should then disappear and $C_{i,j,k}^{(3)\text{sym}}(t_s, t_c, t_p) = 0$ on the lattice, at zero recoil.

Since it must vanish at zero recoil on the lattice, we may subtract from the three-point correlator at non-vanishing recoil the same configuration at zero recoil. This reduces some correlated noise, and indeed it turns out that the signal, although still very noisy, is significantly improved. We have computed the three-point functions with both all μ positive (set sp_0) and all opposite in sign (set sp_1). It turns out that the real parts of the three-point functions are very similar for both sp_0 and sp_1 sets, while the imaginary parts are approximatively opposite in signs, from which we can guess that the contributions with i, j, k not all different are dominantly real, while the ones with i, j, k different are dominantly imaginary. This is related to the fact that the terms odd in the μ have an i with respect to the ones which are

³ We are indebted to Philippe Boucaud who suggested this trick.

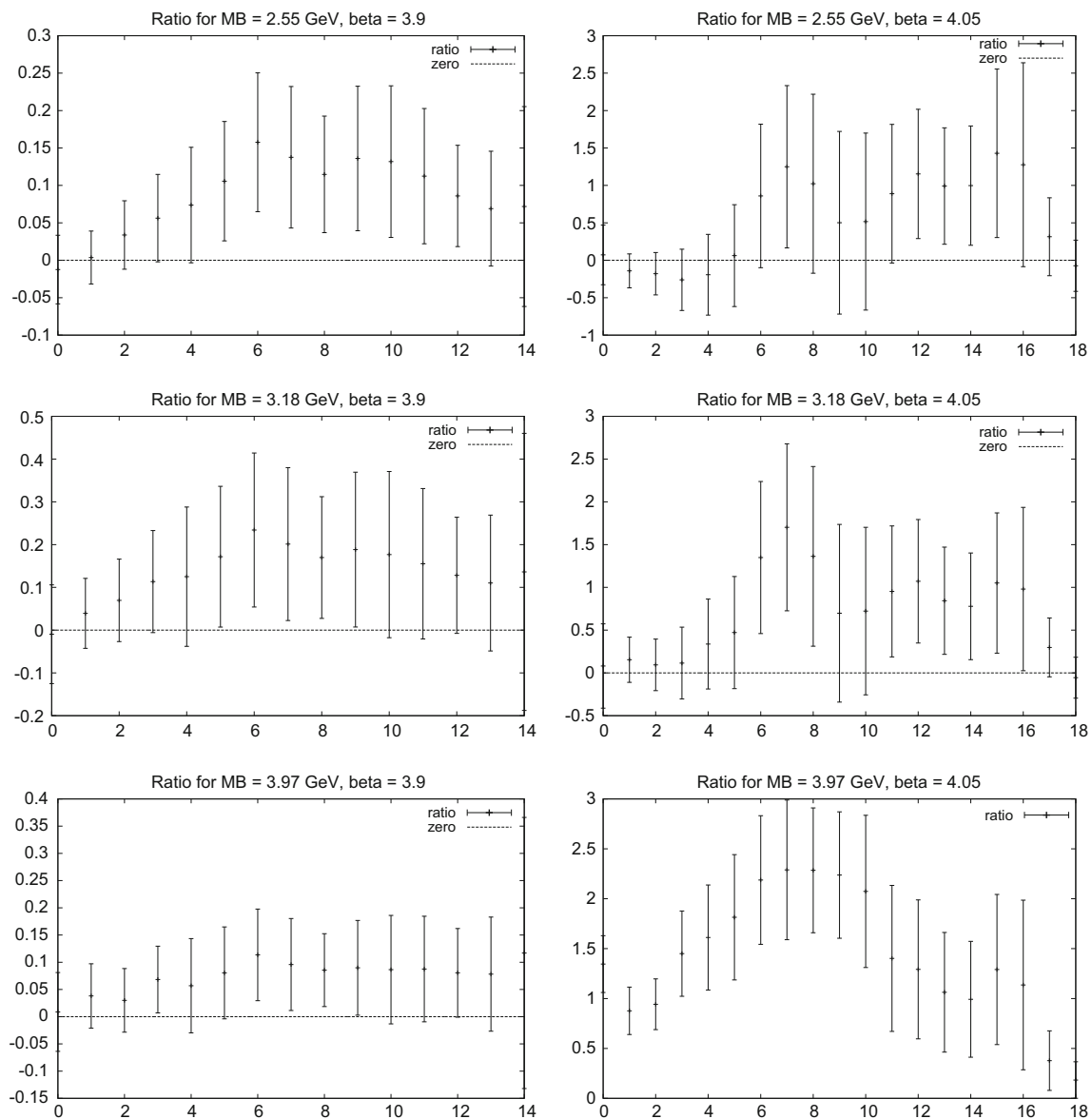


Fig. 7 The ratio of the matrix element for $B \rightarrow D_2^*$ over the value derived from the infinite mass limit, Eq. (6.6), for $w = 1.3$, once the three-point function has been symmetrised according to Eq. (5.11) and once the three-point function at zero recoil has been subtracted. We show the three b quark masses. The plots on the left correspond to $\beta = 3.9$

and $t_p - t_s = 14$, those to the right to $\beta = 4.05$ and $t_p - t_s = 18$. The upper line corresponds to the B meson of continuum mass 2.55 GeV, the second to 3.18 GeV and the third to 3.97 GeV. We use for the three-point functions the average of the combinations expanded in Table 6

even, but for the sake of brevity we will skip an exact proof (Fig. 7).

6.3 Extracting the matrix element

An estimate of $p \tilde{k}$ is thus given by

$$R_{i,D_2^*,\vec{\theta}}(t_p, t, t_s) = \frac{C_{B(\vec{\theta})A_i D_2^*}^{(3)}(t_p, t, t_s) \sqrt{Z_B Z_{D_2^*}} Z_A}{C_{D_2^*}^{(2)}(t - t_s) C_{B(\vec{\theta})}^{(2)}(t_p - t)}, \quad (6.2)$$

where the three-point correlators are the combinations of correlators listed in Table 6, symmetrised according to Eq. (5.11) and with the corresponding zero recoil three-point correlators subtracted. Let us recall that $\vec{p} = \vec{\theta} \pi / L$ where L is the spatial length of the lattice. We have used systematically $\vec{\theta}_x = \vec{\theta}_y = \vec{\theta}_z = \vec{\theta}$ whence $|\vec{p}| = \sqrt{3} \theta \pi / L$. In fact we prefer to present another ratio. Since the estimate of $B \rightarrow D_2^*$ in the infinite mass limit is rather successful, in good agreement with experiment, we will compute the ratio of the three-point correlators divided by the one which is derived from the infinite mass limit formula [8]:

$$\tau_{3/2}(w) = \tau_{3/2}(1) \left(\frac{2}{1+w} \right)^{2\sigma_{3/2}^2}. \quad (6.3)$$

Here the fit gives $\sigma_{3/2}^2 \simeq 1.5$ and $\tau_{3/2}(1) \simeq 0.54$ and the formula in Sect. 2.5.1

$$\tilde{k}_{\text{inf}} = \sqrt{3} \sqrt{r_{D_2^*}} (1+w) \tau_{3/2}(w), \quad (6.4)$$

with $r_{D_2^*} = M_{D_2^*}/M_B$. This \tilde{k}_{inf} will be used as a benchmark for \tilde{k} extracted from our present calculations. From our benchmark \tilde{k}_{inf} we compute the benchmark three-point correlator, the D_2^* meson being created at time t_s the current inserted at time t and the B annihilated at time t_p :

$$C_{\text{inf}}^{(3)}(t_p, t, t_s) = \tilde{k}_{\text{inf}} |\vec{p}| C_{D_2^*}^{(2)}(t - t_s) C_B^{(2)}(t_p - t) Z_A / \sqrt{Z_B Z_{D_2^*}}. \quad (6.5)$$

We thus consider the ratio

$$\frac{\tilde{k}}{\tilde{k}_{\text{inf}}} = \frac{C_{B(\vec{\theta})A_i D_2^*}^{(3)}(t_p, t, t_s)}{C_{\text{inf}}^{(3)}(t_p, t, t_s)}. \quad (6.6)$$

To increase the signal we take the average of the 11 expressions for \tilde{k} in Table 6, for all three masses of the B meson, for $\beta = 3.9$ and $\beta = 4.05$. For the two-point functions in Eq. (6.5) we have used the numerical values. As can be seen all these plots show similar shapes. There is a positive noisy signal, of the order 1 for $\beta = 4.05$. For $\beta = 3.9$ the ratio is about one order of magnitude smaller. We do not understand this feature.

To conclude we may claim that there is a hint of a signal for $B \rightarrow D_2^* \ell \nu$ with finite $m_{c,b}$. But the size of the statistical and systematic errors do not allow us to provide any quantitative result. It is clear that improving the signal is a major goal. This can be performed using larger statistics, using the points at $\beta = 4.2$, using different times for the sink, using other lattice actions and trying to find better interpolating fields.

7 Conclusions and prospects

The major goal of this paper concerned the orbitally excited states of the charmed mesons and the semileptonic decay of the B meson into the latter. We have concentrated on D_2^* and D_0^* (see [39] for a study of the mass spectrum including the spin-1 particles). We have considered three “ B mesons” with, respectively, masses of 2.55, 3.18 and 3.97 GeV. We have used only two lattice spacings, 0.085 and 0.069 fm, with the addition of data with 0.054 fm for D_0^* .

Concerning the spectroscopy, we have noted a discrepancy between the masses of the D_2^* states which are in the E ($D_i V_i$) discrete group and the ones in the T_2 ($D_i V_j$; $j \neq i$).

This is, of course, a lattice artefact. We have also studied the B meson energy as a function of the momentum. There is a clear departure from the theoretical formula for the heaviest meson. This is presumably also an artefact. The D_0^* state can decay into a D meson due to the parity violation when using twisted quarks. It was necessary to use the GEVP method to overcome this difficulty. The mass differences between the D_2^* (D_0^*) with the D meson mass, extrapolated to the continuum, do not agree well with experiment. There are indications that reducing the cut-off effects improves this result.

To compute the form factors and branching fractions we have derived all the needed theoretical formulae necessary to estimate any form factor from lattice calculation.

Concerning $B \rightarrow D_0^*$ we have, up to now, only considered the zero recoil quantity. Our result is that, contrary to the case of infinite b and c masses, the zero recoil amplitude does not vanish. This should increase drastically the ratio of $B \rightarrow D_0^*$ branching fraction over the $B \rightarrow D_2^*$ one, as compared to the infinite mass case. We estimate the ratio of zero recoil amplitudes ($B \rightarrow D_0^* \ell \nu$)/($B \rightarrow D_2^* \ell \nu$) = 0.17(6)(6). The corresponding ratio of branching fractions should be around 0.02, with very large errors. Some experimental semileptonic branching ratios seem to indicate for this ratio a figure of the order of 0.1, but the experimental situation is far from clear and our theoretical estimate still needs much work.

The $B \rightarrow D_2^*$ is treated by a subtraction of the zero recoil contribution which we prove to be theoretically vanishing. There is a signal, although still very noisy. We take the infinite mass result as a benchmark. The ratio to the infinite mass prediction is around 1 for $\beta = 4.05$ but around 0.1 for $\beta = 3.9$, which indicates that beyond the very large statistical errors the systematic effects are not yet well understood.

Altogether, this paper has to be taken as a preliminary study. To our knowledge it is the first study of semileptonic decays to orbitally excited charmed mesons with finite masses for the b and c . The considered process is very noisy and it is already rewarding that we got signals which seem to make sense, although the uncertainty is still much too large.

To improve the situation it seems that the path to follow is to further analyse the data set of ETMC at $\beta = 4.2$ ($a \simeq 0.055$ fm) and check against another lattice regularisation. The extrapolation to the continuum will thus be on a much safer ground. An increase of the statistics might also help.

We also stress that B_s and D_s sectors are presumably interesting to examine. Indeed, the $D_{s0}^*(2317)$ and $D_{s1}^*(2460)$ states stand below the DK and D^*K thresholds: hence they are narrow. At LHCb, according to a phenomenological study [44], about 100 events in the channel $B_s \rightarrow D_{s0}^* \pi^+$ are

expected with 1 fb^{-1} of integrated luminosity. It is an encouragement to extend our effort of measuring the form factors of $B \rightarrow D^{**}$ semileptonic decays in the heavy-strange sector.

Acknowledgments We acknowledge many enlightening discussions with Philippe Boucaud, Francesco Sanfilippo and Marc Wagner. We have intensively used NISAN, the software created by F. Sanfilippo. This work was granted access to the HPC resources of IDRIS under the allocation 2013-052271 made by GENCI. Many calculations were performed on the computing centre or IN2P3 in Lyon. Mariam Atoui acknowledges the “Conseil National de la Recherche Scientifique au Liban (CNRS), Liban” for her thesis grant.

Open Access This article is distributed under the terms of the Creative Commons Attribution 4.0 International License (<http://creativecommons.org/licenses/by/4.0/>), which permits unrestricted use, distribution, and reproduction in any medium, provided you give appropriate credit to the original author(s) and the source, provide a link to the Creative Commons license, and indicate if changes were made. Funded by SCOAP³.

Appendix

Coefficients of the hadronic tensor $W_{\mu\nu}$

In order to compute explicitly the coefficients α , β_{++} , β_{+-} , β_{-+} , β_{--} and γ given in (2.3), we will have to evaluate the possible summation over the D^{**} spins. Scalar meson We have no summation and we get

$$\begin{aligned}\alpha &= 0 & \gamma &= 0, \\ \beta_{++} &= \tilde{u}_+^2 & \beta_{+-} &= \tilde{u}_+ \tilde{u}_- & \beta_{-+} &= \tilde{u}_+ \tilde{u}_-, \\ \beta_{--} &= \tilde{u}_-^2.\end{aligned}$$

Tensor meson We have $J = 2$; the polarisation tensor $\varepsilon_{\mu\nu}^{(p)}$ satisfies [41, 42]:

$$\begin{aligned}\sum_s \varepsilon_{\mu\nu}^{(p)*} \varepsilon_{\rho\sigma}^{(p)} &= -\frac{1}{3} \left(g_{\mu\nu} - \frac{p_\mu p_\nu}{p^2} \right) \left(g_{\rho\sigma} - \frac{p_\rho p_\sigma}{p^2} \right) \\ &+ \frac{1}{2} \left(g_{\mu\rho} - \frac{p_\mu p_\rho}{p^2} \right) \left(g_{\nu\sigma} - \frac{p_\nu p_\sigma}{p^2} \right) \\ &+ \frac{1}{2} \left(g_{\mu\sigma} - \frac{p_\mu p_\sigma}{p^2} \right) \left(g_{\nu\rho} - \frac{p_\nu p_\rho}{p^2} \right).\end{aligned}$$

After calculation, we obtain

$$\begin{aligned}\alpha &= -\frac{(p_B \cdot p_{D_2^*})^2 - m_B^2 m_{D_2^*}^2}{2 m_{D_2^*}^2} \\ &\times \left[\tilde{k}^2 + 4 \tilde{h}^2 \left((p_B \cdot p_{D_2^*})^2 - m_B^2 m_{D_2^*}^2 \right) \right], \\ \beta_{++} &= \frac{2 \tilde{k} \tilde{b}_+}{3 m_{D_2^*}^4} \left((p_B \cdot p_{D_2^*})^2 - m_B^2 m_{D_2^*}^2 \right) \left((p_B \cdot p_{D_2^*})^2 - m_B^2 m_{D_2^*}^2 \right) \\ &+ \frac{2 \tilde{b}_+^2}{3 m_{D_2^*}^4} \left((p_B \cdot p_{D_2^*})^2 - m_B^2 m_{D_2^*}^2 \right)^2 \\ &- \frac{\tilde{h}^2}{2 m_{D_2^*}^2} \left((p_B \cdot p_{D_2^*})^2 - m_B^2 m_{D_2^*}^2 \right) (p_B - p_{D_2^*})^2 \\ &+ \frac{\tilde{k}^2}{24 m_{D_2^*}^4} \left[m_{D_2^*}^2 (p_B - p_{D_2^*})^2 + 4 \left((p_B \cdot p_{D_2^*})^2 - m_B^2 m_{D_2^*}^2 \right) \right], \\ \beta_{+-} &= \beta_{-+} = \frac{2 \tilde{b}_+ \tilde{b}_-}{3 m_{D_2^*}^4} \left((p_B \cdot p_{D_2^*})^2 - m_B^2 m_{D_2^*}^2 \right)^2 \\ &+ \frac{\tilde{k} \tilde{b}_-}{3 m_{D_2^*}^4} (p_B \cdot p_{D_2^*} - m_{D_2^*}^2) \left((p_B \cdot p_{D_2^*})^2 - m_B^2 m_{D_2^*}^2 \right) \\ &- \frac{\tilde{k} \tilde{b}_+}{3 m_{D_2^*}^4} (p_B \cdot p_{D_2^*} + m_{D_2^*}^2) \left((p_B \cdot p_{D_2^*})^2 - m_B^2 m_{D_2^*}^2 \right) \\ &+ \frac{\tilde{h}^2}{2 m_{D_2^*}^2} (m_B^2 - m_{D_2^*}^2) \left((p_B \cdot p_{D_2^*})^2 - m_B^2 m_{D_2^*}^2 \right) \\ &+ \frac{\tilde{k}^2}{24 m_{D_2^*}^4} \left(3 m_B^2 m_{D_2^*}^2 - 4 (p_B \cdot p_{D_2^*})^2 + m_{D_2^*}^4 \right), \\ \beta_{--} &= -\frac{2 \tilde{k} \tilde{b}_-}{3 m_{D_2^*}^4} (p_B \cdot p_{D_2^*} + m_{D_2^*}^2) \left((p_B \cdot p_{D_2^*})^2 - m_B^2 m_{D_2^*}^2 \right) \\ &+ \frac{2 \tilde{b}_-^2}{3 m_{D_2^*}^4} \left((p_B \cdot p_{D_2^*})^2 - m_B^2 m_{D_2^*}^2 \right)^2 \\ &- \frac{\tilde{h}^2}{2 m_{D_2^*}^2} \left((p_B \cdot p_{D_2^*})^2 - m_B^2 m_{D_2^*}^2 \right) (p_B + p_{D_2^*})^2 \\ &+ \frac{\tilde{k}^2}{24 m_{D_2^*}^4} \left[m_{D_2^*}^2 (p_B + p_{D_2^*})^2 + 4 \left((p_B \cdot p_{D_2^*})^2 - m_B^2 m_{D_2^*}^2 \right) \right], \\ \gamma &= \frac{\tilde{k} \tilde{h}}{m_{D_2^*}^2} \left((p_B \cdot p_{D_2^*})^2 - m_B^2 m_{D_2^*}^2 \right).\end{aligned}$$

Variation domains of x and y

First type of constraints: $x = x(y)$

Non-zero mass lepton

We have

$$(m_\ell \neq 0) \quad \left\{ \begin{array}{l} x_{\max} = \frac{1}{2} \left\{ 1 + y - r_{D^{**}}^2 + r_\ell^2 \left[1 + \frac{1}{y} (1 - r_{D^{**}}^2) \right] + \left(1 - \frac{r_\ell^2}{y} \right) \sqrt{[y - (1 - r_{D^{**}})^2][y - (1 + r_{D^{**}})^2]} \right\}, \\ x_{\min} = \frac{1}{2} \left\{ 1 + y - r_{D^{**}}^2 + r_\ell^2 \left[1 + \frac{1}{y} (1 - r_{D^{**}}^2) \right] - \left(1 - \frac{r_\ell^2}{y} \right) \sqrt{[y - (1 - r_{D^{**}})^2][y - (1 + r_{D^{**}})^2]} \right\}, \end{array} \right.$$

with $r_\ell^2 \leq y \leq (1 - r_{D^{**}})^2$.

Zero mass lepton We have

$$(m_\ell = 0) \quad \left\{ \begin{array}{l} x_{\max} = \frac{1}{2} [1 + y - r_{D^{**}}^2 + \sqrt{[y - (1 - r_{D^{**}})^2][y - (1 + r_{D^{**}})^2]}], \\ x_{\min} = \frac{1}{2} [1 + y - r_{D^{**}}^2 - \sqrt{[y - (1 - r_{D^{**}})^2][y - (1 + r_{D^{**}})^2]}], \end{array} \right.$$

with $0 \leq y \leq (1 - r_{D^{**}})^2$.

Second type of constraints: $y = y(x)$

Non-zero mass lepton We have

$$(m_\ell \neq 0) \quad \left\{ \begin{array}{l} y_{\max} = \frac{1}{2} \left[x - \frac{r_{D^{**}}^2 (x - 2r_\ell^2)}{1 - x + r_\ell^2} + \left(1 - \frac{r_{D^{**}}^2}{1 - x + r_\ell^2} \right) \sqrt{x^2 - 4r_\ell^2} \right], \\ y_{\min} = \frac{1}{2} \left[x - \frac{r_{D^{**}}^2 (x - 2r_\ell^2)}{1 - x + r_\ell^2} - \left(1 - \frac{r_{D^{**}}^2}{1 - x + r_\ell^2} \right) \sqrt{x^2 - 4r_\ell^2} \right], \end{array} \right.$$

with $2r_\ell \leq x \leq 1 - r_{D^{**}}^2 + r_\ell^2$.

Zero mass lepton We have

$$(m_\ell = 0) \quad \left\{ \begin{array}{l} y_{\max} = x \left(1 - \frac{r_{D^{**}}^2}{1 - x} \right), \\ y_{\min} = 0, \end{array} \right.$$

with $0 \leq x \leq 1 - r_{D^{**}}^2$.

Expressions for the various decay widths

$\frac{d^2 \Gamma}{dx dy}$ differential decay width

► 3P_0 states

Non-zero mass lepton:

We have

$$\frac{d^2\Gamma}{dx dy} = -\frac{G_F^2 |V_{cb}|^2}{128\pi^3} m_B^5 \left\{ -\tilde{u}_+^2 \left[4 \left[x r_{D_0^*}^2 + (1-x)(y-x) \right] + r_\ell^2 \left[3y - 4(x + r_{D_0^*}^2) + r_\ell^2 \right] \right] \right. \\ \left. + 2 \tilde{u}_+ \tilde{u}_- r_\ell^2 \left[2(1-x-r_{D_0^*}^2) + y + r_\ell^2 \right] \right. \\ \left. + \tilde{u}_-^2 r_\ell^2 (y - r_\ell^2) \right\}.$$

Zero mass lepton: We have

$$\frac{d^2\Gamma}{dx dy} = \frac{G_F^2 |V_{cb}|^2}{32\pi^3} m_B^5 \tilde{u}_+^2 \left[x r_{D_0^*}^2 + (1-x)(y-x) \right].$$

► 3P_2 states

Non-zero mass lepton: We have

$$\frac{d^2\Gamma}{dx dy} = -\frac{m_B}{256\pi^3} \frac{G_F^2 |V_{cb}|^2}{2} \{ C_1 \tilde{k}^2 + C_2 \tilde{h}^2 + C_3 \tilde{b}_+^2 + C_4 \tilde{b}_-^2 + 2 C_5 \tilde{k} \tilde{b}_+ + 2 C_6 \tilde{k} \tilde{b}_- + 2 C_7 \tilde{b}_+ \tilde{b}_- + 2 C_8 \tilde{h} \tilde{k} \}$$

where the C_i coefficients are given by

$$C_1 = \frac{m_B^4}{3 r_{D_2^*}^4} \left\{ \left[y^2 - \left(2 + r_{D_2^*}^2 \right) y + \left(1 - r_{D_2^*}^2 \right)^2 \right] \left[2(1-x)(x-y) + r_{D_2^*}^2 (3y-2x) \right] - 3 y^2 r_{D_2^*}^4 \right. \\ \left. - r_\ell^2 \left[(1-2x+y) \left[2(1-y)^2 - 3 r_{D_2^*}^2 (1+y) \right] - r_{D_2^*}^4 \left(2x - r_{D_2^*}^2 \right) \right] \right. \\ \left. - 2 r_\ell^4 \left[y^2 - 2 \left(1 + r_{D_2^*}^2 \right) y + 1 - r_{D_2^*}^2 + r_{D_2^*}^4 \right] \right\},$$

$$C_2 = \frac{m_B^8}{r_{D_2^*}^2} \left[y - (1 - r_{D_2^*}^2)^2 \right] \left[y - (1 + r_{D_2^*}^2)^2 \right] \\ \times \left[y \left[2(1-x+r_{D_2^*}^2)(1-x-r_{D_2^*}^2) - (1-y+r_{D_2^*}^2)(1+y-2x-r_{D_2^*}^2) \right] \right. \\ \left. + r_\ell^2 \left[(1+y-r_{D_2^*}^2)(1+y-2x-r_{D_2^*}^2) + 2 r_\ell^2 \right] \right],$$

$$C_3 = \frac{m_B^8}{6 r_{D_2^*}^4} \left[y - (1 - r_{D_2^*}^2)^2 \right]^2 \left[y - (1 + r_{D_2^*}^2)^2 \right]^2 \left[4x \left(1 - x - r_{D_2^*}^2 \right) - 4y(1-x) + r_\ell^2 \left[4 \left(x + r_{D_2^*}^2 \right) - 3y - r_\ell^2 \right] \right],$$

$$C_4 = \frac{m_B^8}{6 r_{D_2^*}^4} r_\ell^2 (y - r_\ell^2) \left[y - (1 - r_{D_2^*})^2 \right]^2 \left[y - (1 + r_{D_2^*})^2 \right]^2,$$

$$C_5 = \frac{m_B^6}{3 r_{D_2^*}^4} \left[y - (1 - r_{D_2^*})^2 \right] \left[y - (1 + r_{D_2^*})^2 \right] \\ \times \left[2 \left(1 - y - r_{D_2^*}^2 \right) \left[(1 - x)(x - y) - x r_{D_2^*}^2 \right] - r_\ell^2 \left[\left(1 - y + r_{D_2^*}^2 \right) \left(1 - 3x + 2y - r_{D_2^*}^2 + r_\ell^2 \right) + 2x r_{D_2^*}^2 \right] \right],$$

$$C_6 = \frac{m_B^6}{3 r_{D_2^*}^4} r_\ell^2 \left[y - (1 - r_{D_2^*})^2 \right] \left[y - (1 + r_{D_2^*})^2 \right] \\ \times \left[\left(1 - y + r_{D_2^*}^2 \right) \left(1 - x + r_{D_2^*}^2 \right) + 2 r_{D_2^*}^2 (x - 2) + r_\ell^2 \left(1 - y + r_{D_2^*}^2 \right) \right],$$

$$C_7 = \frac{m_B^8}{6 r_{D_2^*}^4} r_\ell^2 \left[y - (1 - r_{D_2^*})^2 \right]^2 \left[y - (1 + r_{D_2^*})^2 \right]^2 \left[2 \left(1 - x - r_{D_2^*}^2 \right) + y + r_\ell^2 \right],$$

$$C_8 = -\frac{m_B^6}{r_{D_2^*}^2} \left[y - (1 - r_{D_2^*})^2 \right] \left[y - (1 + r_{D_2^*})^2 \right] \left[y \left(1 + y - 2x - r_{D_2^*}^2 \right) + r_\ell^2 \left(1 + y - r_{D_2^*}^2 \right) \right].$$

Zero mass lepton: We notice that the coefficients of C_4 , C_6 and C_7 cancel in this limit, leading to

$$\frac{d^2\Gamma}{dx dy} = -\frac{m_B}{256\pi^3} \frac{G_F^2 |V_{cb}|^2}{2} [C_1 \tilde{k}^2 + C_2 \tilde{h}^2 + C_3 \tilde{b}_+^2 + 2 C_5 \tilde{k} \tilde{b}_+ + 2 C_8 \tilde{h} \tilde{k}]$$

where the C_i coefficients are given by

$$C_1 = \frac{m_B^4}{3 r_{D_2^*}^4} \left[\left[y^2 - \left(2 + r_{D_2^*}^2 \right) y + \left(1 - r_{D_2^*}^2 \right)^2 \right] \left[2(1 - x)(x - y) + r_{D_2^*}^2 (3y - 2x) \right] - 3y^2 r_{D_2^*}^4 \right],$$

$$C_2 = \frac{m_B^8}{r_{D_2^*}^2} \left[y - (1 - r_{D_2^*})^2 \right] \left[y - (1 + r_{D_2^*})^2 \right] \\ \times y \left[2 \left(1 - x + r_{D_2^*}^2 \right) \left(1 - x - r_{D_2^*}^2 \right) - \left(1 - y + r_{D_2^*}^2 \right) \left(1 + y - 2x - r_{D_2^*}^2 \right) \right],$$

$$C_3 = \frac{m_B^8}{6 r_{D_2^*}^4} \left[y - (1 - r_{D_2^*})^2 \right]^2 \left[y - (1 + r_{D_2^*})^2 \right]^2 \left[4x \left(1 - x - r_{D_2^*}^2 \right) - 4y(1 - x) \right],$$

$$C_5 = \frac{m_B^6}{3 r_{D_2^*}^4} \left[y - (1 - r_{D_2^*})^2 \right] \left[y - (1 + r_{D_2^*})^2 \right] \left[2 \left(1 - y - r_{D_2^*}^2 \right) \left[(1 - x)(x - y) - x r_{D_2^*}^2 \right] \right],$$

$$C_8 = -\frac{m_B^6}{r_{D_2^*}^2} \left[y - (1 - r_{D_2^*})^2 \right] \left[y - (1 + r_{D_2^*})^2 \right] y \left(1 + y - 2x - r_{D_2^*}^2 \right).$$

$\frac{d\Gamma}{dy}$ differential decay width

The form factors depend only on the y parameter, but in an unknown way. So, the integration over the x variable can be done through the use the expressions of the type $x = x(y)$.

► 3P_0 states

Non-zero mass lepton: We have

$$\frac{d\Gamma}{dy} = -\frac{G_F^2 |V_{cb}|^2}{128\pi^3} m_B^5 \left[D_1 \tilde{u}_+^2 + 2 D_2 \tilde{u}_+ \tilde{u}_- + D_3 \tilde{u}_-^2 \right]$$

where the D_i coefficients are functions of y and are given by

$$D_1 = \frac{1}{3y^3} (y - r_\ell^2)^2 \left[\left[y - (1 - r_{D_0^*}^2) \right] \left[y - (1 + r_{D_0^*}^2) \right] \right]^{1/2} \\ \times \left\{ 2y \left[y - (1 - r_{D_0^*}^2) \right] \left[y - (1 + r_{D_0^*}^2) \right] + r_\ell^2 \left[y^2 - 2y \left(1 + r_{D_0^*}^2 \right) + 4 \left(1 - r_{D_0^*}^2 \right)^2 \right] \right\},$$

$$D_2 = \frac{1}{y^2} r_\ell^2 (y - r_\ell^2)^2 \left(1 - r_{D_0^*}^2 \right) \left[\left[y - (1 - r_{D_0^*}^2) \right] \left[y - (1 + r_{D_0^*}^2) \right] \right]^{1/2},$$

$$D_3 = \frac{1}{y} r_\ell^2 (y - r_\ell^2)^2 \left[\left[y - (1 - r_{D_0^*}^2) \right] \left[y - (1 + r_{D_0^*}^2) \right] \right]^{1/2}.$$

Let us recall that, in that expression of $d\Gamma/dy$, the y parameter belongs in the interval: $r_\ell^2 \leq y \leq (1 - r_{D_0^*}^2)^2$

Zero mass lepton: We have

$$\frac{d\Gamma}{dy} = -\frac{G_F^2 |V_{cb}|^2}{128\pi^3} m_B^5 \tilde{u}_+^2 D_1 \quad \text{where} \quad D_1 = \frac{2}{3} \left[\left[y - (1 - r_{D_0^*}^2) \right] \left[y - (1 + r_{D_0^*}^2) \right] \right]^{3/2},$$

since the other coefficients, D_2 and D_3 , give zero in this case.

► 3P_2 states

Non-zero mass lepton: We have

$$\frac{d\Gamma}{dy} = -\frac{m_B}{256\pi^3} \frac{G_F^2 |V_{cb}|^2}{2} \{ D_1 \tilde{k}^2 + D_2 \tilde{h}^2 + D_3 \tilde{b}_+^2 + D_4 \tilde{b}_-^2 + 2 D_5 \tilde{k} \tilde{b}_+ + 2 D_6 \tilde{k} \tilde{b}_- + 2 D_7 \tilde{b}_+ \tilde{b}_- + 2 D_8 \tilde{h} \tilde{k} \}$$

where the D_i coefficients are given by

$$D_1 = \frac{m_B^4}{r_{D_2^*}^4} \frac{1}{9y^3} (y - r_\ell^2)^2 \left[\left[y - (1 - r_{D_2^*})^2 \right] \left[y - (1 + r_{D_2^*})^2 \right] \right]^{3/2} \\ \times \left\{ y \left[y^2 - 2y \left(1 - 4r_{D_2^*}^2 \right) + \left(1 - r_{D_2^*}^2 \right)^2 \right] + r_\ell^2 \left[2y^2 - y \left(4 - r_{D_2^*}^2 \right) + 2 \left(1 - r_{D_2^*}^2 \right)^2 \right] \right\},$$

$$D_2 = \frac{m_B^8}{r_{D_2^*}^2} \frac{1}{3y^2} (y - r_\ell^2)^2 (2y + r_\ell^2) \left[\left[y - (1 - r_{D_2^*})^2 \right] \left[y - (1 + r_{D_2^*})^2 \right] \right]^{5/2},$$

$$D_3 = \frac{m_B^8}{r_{D_2^*}^4} \frac{1}{18y^3} (y - r_\ell^2)^2 \left[\left[y - (1 - r_{D_2^*})^2 \right] \left[y - (1 + r_{D_2^*})^2 \right] \right]^{5/2} \\ \times \left\{ 2y \left[y - (1 - r_{D_2^*})^2 \right] \left[y - (1 + r_{D_2^*})^2 \right] + r_\ell^2 \left[y^2 - 2y \left(1 + r_{D_2^*}^2 \right) + 4 \left(1 - r_{D_2^*}^2 \right)^2 \right] \right\},$$

$$D_4 = \frac{m_B^8}{r_{D_2^*}^4} \frac{1}{6y} r_\ell^2 (y - r_\ell^2)^2 \left[\left[y - (1 - r_{D_2^*})^2 \right] \left[y - (1 + r_{D_2^*})^2 \right] \right]^{5/2},$$

$$D_5 = \frac{m_B^6}{r_{D_2^*}^4} \frac{1}{18y^3} (y - r_\ell^2)^2 \left[\left[y - (1 - r_{D_2^*})^2 \right] \left[y - (1 + r_{D_2^*})^2 \right] \right]^{5/2} \left[2y \left(1 - y - r_{D_2^*}^2 \right) + r_\ell^2 \left(4 - y - 4r_{D_2^*}^2 \right) \right],$$

$$D_6 = \frac{m_B^6}{r_{D_2^*}^4} \frac{1}{6y^2} r_\ell^2 (y - r_\ell^2)^2 \left[\left[y - (1 - r_{D_2^*})^2 \right] \left[y - (1 + r_{D_2^*})^2 \right] \right]^{5/2},$$

$$D_7 = \frac{m_B^8}{r_{D_2^*}^4} \frac{1}{6y^2} r_\ell^2 (y - r_\ell^2)^2 \left(1 - r_{D_2^*}^2 \right) \left[\left[y - (1 - r_{D_2^*})^2 \right] \left[y - (1 + r_{D_2^*})^2 \right] \right]^{5/2},$$

$$D_8 = 0.$$

We recall that, in those formulae, the y parameter varies inside the domain $r_\ell^2 \leq y \leq (1 - r_{D_2^*})^2$

Zero mass lepton: We have

$$\frac{d\Gamma}{dy} = - \frac{m_B}{256\pi^3} \frac{G_F^2 |V_{cb}|^2}{2} [D_1 \tilde{k}^2 + D_2 \tilde{h}^2 + D_3 \tilde{b}_+^2 + 2 D_5 \tilde{k} \tilde{b}_+ + 2 D_8 \tilde{h} \tilde{k}]$$

where the D_i coefficients are given by

$$D_1 = \frac{m_B^4}{r_{D_2^*}^4} \frac{1}{9} \left[\left[y - (1 - r_{D_2^*})^2 \right] \left[y - (1 + r_{D_2^*})^2 \right] \right]^{3/2} \left[y^2 - 2y \left(1 - 4r_{D_2^*}^2 \right) + \left(1 - r_{D_2^*}^2 \right)^2 \right],$$

$$D_2 = \frac{m_B^8}{r_{D_2^*}^2} \frac{2}{3} y \left[\left[y - (1 - r_{D_2^*})^2 \right] \left[y - (1 + r_{D_2^*})^2 \right] \right]^{5/2},$$

$$D_3 = \frac{m_B^8}{r_{D_2^*}^4} \frac{1}{9} \left[\left[y - (1 - r_{D_2^*})^2 \right] \left[y - (1 + r_{D_2^*})^2 \right] \right]^{7/2},$$

$$D_5 = \frac{m_B^6}{r_{D_2^*}^4} \frac{1}{9} (1 - y - r_{D_2^*}^2) \left[\left[y - (1 - r_{D_2^*})^2 \right] \left[y - (1 + r_{D_2^*})^2 \right] \right]^{5/2},$$

$$D_8 = 0.$$

Here, the y parameter lies in the domain $0 \leq y \leq (1 - r_{D_2^*})^2$.

$\frac{d\Gamma}{dx}$ differential decay width

It is impossible to give general expressions for the leptonic spectra $\frac{d\Gamma}{dx}$, since the integration over y cannot be performed because we do not know the dependence of the form factors on y .

Nevertheless, the procedure to do those calculations is the following:

1. We start from the expressions of the $\frac{d^2\Gamma}{dx dy}$ decay widths given above.
2. We use the constraints of the type $y = y(x)$ in order to perform the integration over y from y_{\min} to y_{\max} (expressions given also above). Incidentally, we must not forget that the maximum of $E_{D^{**}}$ corresponds to the minimum of y and vice versa. So, to integrate over $E_{D^{**}}$ from $E_{D^{**}}^{\min}$ to $E_{D^{**}}^{\max}$, we have to integrate equivalently over y from y_{\max} to y_{\min} :

$$\frac{d\Gamma}{dx} = \int_{y_{\max}}^{y_{\min}} \frac{d^2\Gamma}{dx dy} dy$$

with

$$\begin{cases} y_{\max} = \frac{1}{2} \left[x - \frac{r_{D^{**}}^2 (x - 2r_\ell^2)}{1 - x + r_\ell^2} + \left(1 - \frac{r_{D^{**}}^2}{1 - x + r_\ell^2} \right) \sqrt{x^2 - 4r_\ell^2} \right], \\ y_{\min} = \frac{1}{2} \left[x - \frac{r_{D^{**}}^2 (x - 2r_\ell^2)}{1 - x + r_\ell^2} - \left(1 - \frac{r_{D^{**}}^2}{1 - x + r_\ell^2} \right) \sqrt{x^2 - 4r_\ell^2} \right]. \end{cases}$$

$r_\ell = 0$ gives the relations in the case of a zero mass lepton.

3. The last free parameter x lies in the domain

$$2r_\ell \leq x \leq 1 - r_{D^{**}}^2 + r_\ell^2.$$

Once again, $r_\ell = 0$ gives the variation domain in the case of a zero mass lepton.

Total decay width Γ

The problem, mentioned for the leptonic spectra, pops up here again because, in order to get Γ , we will have to integrate over y at some point. So we will have to follow the same procedure.

Polarisation tensor for the 3P_2 state

Using expressions for the spin-1 polarisation vector found in [43] for instance and the values of the Clebsch–Gordan coefficient from the Particle Physics Booklet, we get

$$\begin{aligned} \varepsilon_{(+2)}^{\mu\nu} &= \frac{1}{2} \begin{pmatrix} 0 & 0 & 0 & 0 \\ 0 & 1 & i & 0 \\ 0 & i & -1 & 0 \\ 0 & 0 & 0 & 0 \end{pmatrix}, & \varepsilon_{(-2)}^{\mu\nu} &= \frac{1}{2} \begin{pmatrix} 0 & 0 & 0 & 0 \\ 0 & 1 & -i & 0 \\ 0 & -i & -1 & 0 \\ 0 & 0 & 0 & 0 \end{pmatrix}, \\ \varepsilon_{(+1)}^{\mu\nu} &= \frac{1}{2} \begin{pmatrix} 0 & 0 & 0 & 0 \\ 0 & 0 & 0 & -1 \\ 0 & 0 & 0 & -i \\ 0 & -1 & -i & 0 \end{pmatrix}, \\ \varepsilon_{(-1)}^{\mu\nu} &= \frac{1}{2} \begin{pmatrix} 0 & 0 & 0 & 0 \\ 0 & 0 & 0 & 1 \\ 0 & 0 & 0 & -i \\ 0 & 1 & -i & 0 \end{pmatrix}, & \varepsilon_{(0)}^{\mu\nu} &= \frac{1}{\sqrt{6}} \begin{pmatrix} 0 & 0 & 0 & 0 \\ 0 & -1 & 0 & 0 \\ 0 & 0 & -1 & 0 \\ 0 & 0 & 0 & 2 \end{pmatrix}. \end{aligned}$$

We dropped the $\vec{0}$ in the notation.

Extraction of the form factors

The following expressions are not exhaustive.

Note that it is possible to recover the momentum transfer $y m_B^2 = (p_B - p_{D^{**}})^2$ using

$$E_B = \frac{m_B}{2r_{D^{**}}} [1 - y + r_{D^{**}}^2] \quad \text{and} \quad p^2 \\ = \frac{m_B^2}{12r_{D^{**}}^2} [y - (1 - r_{D^{**}})^2] [y - (1 + r_{D^{**}})^2],$$

leading to

$$E_B + m_{D^{**}} = \frac{m_B}{2r_{D^{**}}} (1 - y + 3r_{D^{**}}^2) \\ E_B - m_{D^{**}} = \frac{m_B}{2r_{D^{**}}} (1 - y - r_{D^{**}}^2).$$

 3P_0 form factors

With $\mathcal{T}_\mu^A \stackrel{\text{def.}}{=} \langle {}^3P_0 A_\mu B(p_B) \rangle$:

• form factor \tilde{u}_+

$$\tilde{u}_+ = -\frac{1}{2m_{D^{**}}} \left[\frac{E_B - m_{D^{**}}}{p} \mathcal{T}_i^A - \mathcal{T}_0^A \right] \\ = -\frac{1}{2m_{D^{**}}} \left[\frac{E_B - m_{D^{**}}}{3p} (\mathcal{T}_1^A + \mathcal{T}_2^A + \mathcal{T}_3^A) - \mathcal{T}_0^A \right],$$

• form factor \tilde{u}_-

$$\tilde{u}_- = \frac{1}{2m_{D^{**}}} \left[\frac{E_B + m_{D^{**}}}{p} \mathcal{T}_i^A - \mathcal{T}_0^A \right] \\ = \frac{1}{2m_{D^{**}}} \left[\frac{E_B + m_{D^{**}}}{3p} (\mathcal{T}_1^A + \mathcal{T}_2^A + \mathcal{T}_3^A) - \mathcal{T}_0^A \right].$$

 3P_2 form factors

With $\mathcal{T}_{\mu(\lambda)}^A \stackrel{\text{def.}}{=} \langle {}^3P_2(\lambda) | A_\mu | B(p_B) \rangle$ and $\mathcal{T}_{\mu(\lambda)}^V \stackrel{\text{def.}}{=} \langle {}^3P_2(\lambda) V_\mu B(p_B) \rangle$:

• form factor \tilde{k}

$$\tilde{k} = -\frac{\sqrt{6}}{p} \mathcal{T}_{1(0)}^A = -\frac{\sqrt{6}}{p} \mathcal{T}_{2(0)}^A = \frac{\sqrt{6}}{2p} \mathcal{T}_{3(0)}^A \\ = \frac{1}{p} [\mathcal{T}_{1(+2)}^A + \mathcal{T}_{1(-2)}^A] = -\frac{1}{p} [\mathcal{T}_{2(+2)}^A + \mathcal{T}_{2(-2)}^A],$$

• form factors \tilde{b}_+ and \tilde{b}_-

$$\begin{cases} \tilde{b}_+ = -\frac{1+i}{4} \frac{1}{p^3 m_{D^{**}}} [(E_B - m_{D^{**}})(i \mathcal{T}_{1(+2)}^A + \mathcal{T}_{2(+2)}^A) \\ \quad - p(1+i) \mathcal{T}_{0(+2)}^A], \\ \tilde{b}_- = \frac{1+i}{4} \frac{1}{p^3 m_{D^{**}}} [(E_B + m_{D^{**}})(i \mathcal{T}_{1(+2)}^A + \mathcal{T}_{2(+2)}^A) \\ \quad - p(1+i) \mathcal{T}_{0(+2)}^A], \end{cases} \\ \begin{cases} \tilde{b}_+ = \frac{1-i}{4} \frac{1}{p^3 m_{D^{**}}} [(E_B - m_{D^{**}})(i \mathcal{T}_{1(-2)}^A - \mathcal{T}_{2(-2)}^A) \\ \quad + p(1-i) \mathcal{T}_{0(-2)}^A], \\ \tilde{b}_- = -\frac{1-i}{4} \frac{1}{p^3 m_{D^{**}}} [(E_B + m_{D^{**}})(i \mathcal{T}_{1(-2)}^A - \mathcal{T}_{2(-2)}^A) \\ \quad + p(1-i) \mathcal{T}_{0(-2)}^A], \end{cases} \\ \begin{cases} \tilde{b}_+ = \frac{1+i}{4} \frac{1}{p^3 m_{D^{**}}} [(E_B - m_{D^{**}})(\mathcal{T}_{1(+1)}^A + \mathcal{T}_{2(+1)}^A) \\ \quad - \mathcal{T}_{3(+1)}^A - p \mathcal{T}_{0(+1)}^A], \\ \tilde{b}_- = -\frac{1+i}{4} \frac{1}{p^3 m_{D^{**}}} [(E_B + m_{D^{**}})(\mathcal{T}_{1(+1)}^A + \mathcal{T}_{2(+1)}^A) \\ \quad - \mathcal{T}_{3(+1)}^A - p \mathcal{T}_{0(+1)}^A], \end{cases} \\ \begin{cases} \tilde{b}_+ = -\frac{1-i}{4} \frac{1}{p^3 m_{D^{**}}} [(E_B - m_{D^{**}})(\mathcal{T}_{1(-1)}^A + \mathcal{T}_{2(-1)}^A) \\ \quad - \mathcal{T}_{3(-1)}^A - p \mathcal{T}_{0(-1)}^A], \\ \tilde{b}_- = \frac{1-i}{4} \frac{1}{p^3 m_{D^{**}}} [(E_B + m_{D^{**}})(\mathcal{T}_{1(-1)}^A + \mathcal{T}_{2(-1)}^A) \\ \quad - \mathcal{T}_{3(-1)}^A - p \mathcal{T}_{0(-1)}^A], \end{cases} \\ \begin{cases} \tilde{b}_+ = \frac{1}{2i} \frac{1}{p^3 m_{D^{**}}} [(E_B - m_{D^{**}})(\mathcal{T}_{3(+2)}^A - p \mathcal{T}_{0(+2)}^A)], \\ \tilde{b}_- = \frac{1}{2i} \frac{1}{p^3 m_{D^{**}}} [-(E_B + m_{D^{**}})(\mathcal{T}_{3(+2)}^A + p \mathcal{T}_{0(+2)}^A)], \end{cases}$$

• form factor \tilde{h}

$$\tilde{h} = \frac{1}{2i} \frac{1}{p m_{D^{**}}} \frac{\mathcal{T}_{1(\lambda)}^V}{\varepsilon_{(\lambda)}^{*3\alpha} p_{B\alpha} - \varepsilon_{(\lambda)}^{*2\alpha} p_{B\alpha}} \\ = \frac{1}{2i} \frac{1}{p m_{D^{**}}} \frac{\mathcal{T}_{2(\lambda)}^V}{\varepsilon_{(\lambda)}^{*1\alpha} p_{B\alpha} - \varepsilon_{(\lambda)}^{*3\alpha} p_{B\alpha}} \\ = -\frac{1}{2i} \frac{1}{p m_{D^{**}}} \frac{\mathcal{T}_{3(\lambda)}^V}{\varepsilon_{(\lambda)}^{*2\alpha} p_{B\alpha} - \varepsilon_{(\lambda)}^{*1\alpha} p_{B\alpha}}$$

where

λ	$\varepsilon_{(\lambda)}^{*3\alpha} p_{B\alpha} - \varepsilon_{(\lambda)}^{*2\alpha} p_{B\alpha}$	$\varepsilon_{(\lambda)}^{*1\alpha} p_{B\alpha} - \varepsilon_{(\lambda)}^{*3\alpha} p_{B\alpha}$	$\varepsilon_{(\lambda)}^{*2\alpha} p_{B\alpha} - \varepsilon_{(\lambda)}^{*1\alpha} p_{B\alpha}$
+2	$-\frac{p}{2}(1+i)$	$-\frac{p}{2}(1-i)$	p
+1	$\frac{p}{2}$	$i\frac{p}{2}$	$-\frac{p}{2}(1+i)$
0	$-p\sqrt{\frac{3}{2}}$	$p\sqrt{\frac{3}{2}}$	0
-1	$-\frac{p}{2}$	$i\frac{p}{2}$	$\frac{p}{2}(1-i)$
-2	$-\frac{p}{2}(1-i)$	$-\frac{p}{2}(1+i)$	p

Masses and energies

We collect in Table 7 the masses and energies that we extract in our analysis.

Table 7 Masses and energies extracted from the two-point correlation functions in units of the lattice spacing. At $\beta = 3.9$, time intervals for the fits are [8, 23] (D), [6, 9] (D_0^* and D_2^*), [11, 17] (small momenta, $B(\mu_{h_1})$ and $B(\mu_{h_2})$), [9, 15] (large momenta, $B(\mu_{h_1})$ and $B(\mu_{h_2})$) and [9, 13] ($B(\mu_{h_3})$). At $\beta = 4.05$, time ranges for the fits are [10, 26] (D), [7, 11] (D_0^* and D_2^*), [14, 26] (small momenta, $B(\mu_{h_1})$ and $B(\mu_{h_2})$), [9, 26] (large momenta, $B(\mu_{h_1})$ and $B(\mu_{h_2})$), [14, 22] (small momenta, $B(\mu_{h_3})$) and [9, 22] (large momenta, $B(\mu_{h_3})$). $\beta = 4.2$ has been added to study the zero recoil decay $B \rightarrow D_0^*$. The windows are [11, 20] (D), [11, 17] (D_0^*) and [13, 20] (B mesons at rest)

Meson	$\beta = 3.9$		$\beta = 4.05$		$\beta = 4.2$	
	θ	$E(\theta)$	θ	$E(\theta)$	θ	$E(\theta)$
D	0	0.76 (1)	0	0.62 (1)	0	0.52 (1)
D_0^*	0	1.01 (4)	0	0.80 (2)	0	0.66 (1)
D_2^*	0	1.14 (2)	0	0.93 (2)	–	–
$B(\mu_{h_1})$	0	1.00 (1)	0	0.82 (1)	0	0.69 (1)
$B(\mu_{h_2})$	0	1.21 (1)	0	1.01 (1)	0	0.85 (1)
$B(\mu_{h_3})$	0	1.50 (1)	0	1.25 (1)	0	1.05 (1)
$B(\mu_{h_1})$	0.99	1.02 (1)	1.09	0.84 (1)		
$B(\mu_{h_2})$	1.21	1.24 (1)	1.35	1.02 (1)		
$B(\mu_{h_3})$	1.48	1.51 (1)	1.67	1.26 (1)		
$B(\mu_{h_1})$	1.41	1.04 (1)	1.56	0.85 (1)		
$B(\mu_{h_2})$	1.72	1.26 (1)	1.92	1.04 (1)		
$B(\mu_{h_3})$	2.11	1.52 (1)	2.37	1.28 (1)		
$B(\mu_{h_1})$	2.02	1.08 (1)	2.23	0.89 (1)		
$B(\mu_{h_2})$	2.46	1.30 (1)	2.74	1.08 (1)		
$B(\mu_{h_3})$	3.01	1.55 (1)	3.39	1.31 (1)		
$B(\mu_{h_1})$	2.50	1.12 (1)	2.76	0.92 (2)		
$B(\mu_{h_2})$	3.05	1.34 (1)	3.40	1.11 (2)		
$B(\mu_{h_3})$	3.73	1.58 (1)	4.21	1.34 (1)		
$B(\mu_{h_1})$	2.92	1.16 (1)	3.23	0.95 (2)		
$B(\mu_{h_2})$	3.56	1.38 (1)	3.97	1.15 (2)		
$B(\mu_{h_3})$	4.36	1.60 (2)	4.91	1.38 (2)		
$B(\mu_{h_1})$	3.66	1.25 (1)	4.04	1.00 (3)		
$B(\mu_{h_2})$	4.46	1.46 (1)	4.97	1.22 (3)		
$B(\mu_{h_3})$	5.46	1.66 (2)	6.15	1.45 (1)		

References

1. K.A. Olive et al. [Particle Data Group Collaboration], Chin. Phys. C **38**, 090001 (2014)
2. P. Gambino, T. Mannel, N. Uraltsev, $B \rightarrow D^*$ zero-recoil form-factor and the heavy quark expansion in QCD: a systematic study. JHEP **1210**, 169 (2012). [arXiv:1206.2296](#) [hep-ph]
3. I.I. Bigi, B. Blossier, A. Le Yaouanc, L. Oliver, O. Pene, J.-C. Raynal, A. Oyanguren, P. Roudeau, Memorino on the '1/2 vs. 3/2 puzzle' in $\bar{B} \rightarrow \ell \bar{\nu} X(c)$: a year later and a bit wiser. Eur. Phys. J. C **52**, 975 (2007). [arXiv:0708.1621](#) [hep-ph]
4. A. Le Yaouanc, O. Pene. [arXiv:1408.5104](#) [hep-ph]
5. P. del Amo Sanchez et al. [BaBar Collaboration], Observation of new resonances decaying to $D\pi$ 10.58 GeV. Phys. Rev. D **82**, 111101 (2010). [arXiv:1009.2076](#) [hep-ex]
6. A. Le Yaouanc, L. Oliver, O. Pene, J.C. Raynal, New heavy quark limit sum rules involving Isgur–Wise functions and decay constants. Phys. Lett. B **387**, 582 (1996). [arXiv:hep-ph/9607300](#)
7. N. Uraltsev, New exact heavy quark sum rules. Phys. Lett. B **501**, 86 (2001). [arXiv:hep-ph/0011124](#)
8. V. Morenas, A. Le Yaouanc, L. Oliver, O. Pene, J.C. Raynal, Quantitative predictions for B in quark models a la Bakamjian–Thomas. Phys. Rev. D **56**, 5668 (1997). [arXiv:hep-ph/9706265](#)
9. D. Ebert, R.N. Faustov, V.O. Galkin, Exclusive semileptonic decays of B mesons in the relativistic quark model. Phys. Lett. B **434**, 365 (1998). [arXiv:hep-ph/9805423](#)
10. D. Ebert, R.N. Faustov, V.O. Galkin, Heavy quark $1/m_Q$ mesons. Phys. Rev. D **61**, 014016 (2000). [arXiv:hep-ph/9906415](#)
11. D. Becirevic, B. Blossier, P. Boucaud, G. Herdoiza, J.P. Leroy, A. Le Yaouanc, V. Morenas, O. Pene, Lattice measurement of the Isgur–Wise functions $\tau_{1/2}$. Phys. Lett. B **609**, 298 (2005). [arXiv:hep-lat/0406031](#)
12. B. Blossier et al. [European Twisted Mass Collaboration], Lattice calculation of the Isgur–Wise functions $\tau_{1/2}$ with dynamical quarks. JHEP **0906**, 022 (2009). [arXiv:0903.2298](#) [hep-lat]
13. N. Isgur, M.B. Wise, Excited charm mesons in semileptonic \bar{B} decay and their contributions to a Bjorken sum rule. Phys. Rev. D **43**, 819 (1991)
14. B. Bakamjian, L.H. Thomas, Phys. Rev. **92**, 1300 (1953)
15. N. Isgur, D. Scora, B. Grinstein, M.B. Wise, Semileptonic B and D decays in the quark model. Phys. Rev. D **39**, 799 (1989)
16. P. Boucaud et al. [ETM Collaboration], Dynamical twisted mass fermions with light quarks. Phys. Lett. B **650**, 304 (2007). [arXiv:hep-lat/0701012](#)
17. C. Urbach [European Twisted Mass Collaboration], Lattice QCD with two light Wilson quarks and maximally twisted mass. PoS LAT 022 (2007). [arXiv:0710.1517](#) [hep-lat]
18. P. Boucaud et al. [ETM Collaboration], Dynamical twisted mass fermions with light quarks: simulation and analysis details. Comput. Phys. Commun. **179**, 695 (2008). [arXiv:0803.0224](#) [hep-lat]
19. B. Blossier et al. [ETM Collaboration], Average up/down, strange and charm quark masses with $N_f = 2$ twisted mass lattice QCD. Phys. Rev. D **82**, 114513 (2010). [arXiv:1010.3659](#) [hep-lat]
20. B. Blossier et al. [ETM Collaboration], Ghost-gluon coupling, power corrections and $\Lambda_{\overline{MS}}$. Phys. Rev. D **82**, 034510 (2010). [arXiv:1005.5290](#) [hep-lat]
21. P. Weisz, Continuum limit improved lattice action for pure Yang–Mills theory. I. Nucl. Phys. B **212**, 1 (1983)
22. R. Frezzotti et al. [Alpha Collaboration], Lattice QCD with a chirally twisted mass term. JHEP **0108**, 058 (2001). [arXiv:hep-lat/0101001](#)
23. R. Frezzotti, G.C. Rossi, Chirally improving Wilson fermions. 1. $O(a)$ improvement. JHEP **0408**, 007 (2004). [arXiv:hep-lat/0306014](#)
24. A. Shindler, Twisted mass lattice QCD. Phys. Rep. **461**, 37 (2008). [arXiv:0707.4093](#) [hep-lat]
25. K. Jansen, C. Liu, M. Luscher, H. Simma, S. Sint, R. Sommer, P. Weisz, U. Wolff, Nonperturbative renormalization of lattice QCD at all scales. Phys. Lett. B **372**, 275 (1996). [arXiv:hep-lat/9512009](#)
26. J. Foley, K.J. Juge, A. O’Cais, M. Peardon, S.M. Ryan, J.-I. Skullerud, Practical all-to-all propagators for lattice QCD. Comput. Phys. Commun. **172**, 145 (2005). [arXiv:hep-lat/0505023](#)
27. M. Foster et al. [UKQCD Collaboration], Hadrons with a heavy color adjoint particle. Phys. Rev. D **59**, 094509 (1999). [arXiv:hep-lat/9811010](#)

28. C. McNeile et al. [UKQCD Collaboration], Decay width of light quark hybrid meson from the lattice. Phys. Rev. D **73**, 074506 (2006). [arXiv:hep-lat/0603007](#)
29. S. Gusken, U. Low, K.H. Mutter, R. Sommer, A. Patel, K. Schilling, Nonsinglet axial vector couplings of the baryon octet in lattice QCD. Phys. Lett. B **227**, 266 (1989)
30. M. Albanese et al. [APE Collaboration], Glueball masses and string tension in lattice QCD. Phys. Lett. B **192**, 163 (1987)
31. N. Carrasco et al. [ETM Collaboration], PoS LATTICE **2012**, 105 (2012). [arXiv:1211.0565](#) [hep-lat]
32. R. Frezzotti et al. [ETM Collaboration], Electromagnetic form factor of the pion from twisted-mass lattice QCD at $N_f = 2$. Phys. Rev. D **79**, 074506 (2009). [arXiv:0812.4042](#) [hep-lat]
33. P. Lacey et al. [UKQCD Collaboration], Orbitally excited and hybrid mesons from the lattice. Phys. Rev. D **54**, 6997 (1996). [arXiv:hep-lat/9605025](#)
34. C. Michael, Adjoint sources in lattice gauge theory. Nucl. Phys. B **259**, 58 (1985)
35. M. Luscher, U. Wolff, How to calculate the elastic scattering matrix in two-dimensional quantum field theories by numerical simulation. Nucl. Phys. B **339**, 222 (1990)
36. B. Blossier, M. Della Morte, G. von Hippel, T. Mendes, R. Sommer, On the generalized eigenvalue method for energies and matrix elements in lattice field theory. JHEP **0904**, 094 (2009). [arXiv:0902.1265](#) [hep-lat]
37. A.K. Leibovich, Z. Ligeti, I.W. Stewart, M.B. Wise, Semileptonic B decays to excited charmed mesons. Phys. Rev. D **57**, 308 (1998). [arXiv:hep-ph/9705467](#)
38. B. Blossier et al. [ALPHA Collaboration], JHEP **1012**, 039 (2010). [arXiv:1006.5816](#) [hep-lat]
39. M. Wagner, M. Kalinowski, Twisted mass lattice computation of charmed mesons with focus on D^{**} . [arXiv:1310.5513](#) [hep-lat]
40. D. Mohler, S. Prelovsek, R.M. Woloshyn, Phys. Rev. D **87**(3), 034501 (2013). [arXiv:1208.4059](#) [hep-lat]
41. D. Spehler, S.F. Novaes, Helicity wave functions for massless and massive spin-2 particles. Phys. Rev. D **44**, 3990 (1991)
42. S.Y. Choi, J. Lee, J.S. Shim, H.S. Song, Spin-2 particle polarization. J. Korean Phys. Soc. **25**, 576 (1992)
43. S. Weinberg, *The Quantum Theory of Fields. Vol. 1: Foundations* (Univ. Pr., Cambridge, 1995), p. 609
44. D. Becirevic, A. Le Yaouanc, L. Oliver, J.C. Raynal, P. Roudeau, J. Serrano, Phys. Rev. D **87**(5), 054007 (2013). [arXiv:1206.5869](#) [hep-ph]